BTS RESEARCH

# Non-GLP Drug Discovery Research Services

Phone: (858) 605-5882
Toll Free: (866) 599-3019
Fax: (858) 605-5916

www.btsresearch.com


# IN VITRO ASSAYS

# IN VITRO ASSAYS

Assay development is a crucial step in the process of drug screening against pharmacological targets. This requires expertise in using a broad array of assay technologies and developing reliable and efficient screening assays. BTS Research has developed a wide variety of assay technologies such as:

- Proliferation (Peripheral blood cells, primary cell and cell lines)
- Cytotoxicity
- Cytokine Release
- FACS analysis
- Western Blots/Immunoprecipitation
- Angiogenesis
- Calcium flux
- Intracellular pH flux
- Shape change
- Multiplex assays
- Chemotaxis
- ELISA (human, mouse rat, swine, dog, and primate)
- Cell proliferation and growth inhibition assays (tumor and endothelial cells)
- Apoptosis assays (tumor and endothelial cells)
- HUVEC assays
- RBC lysis assays
- B cell, T cell, monocyte, neutrophils, eosinophis/mast cell and platelet functional assays
- Cell cycle and apoptosis analysis using flow cytometry
- Migration and invasion assays (Matrigel® and fibrin gel)
- Receptor binding and activity assays (ER, PR, AR, PPAR, etc.)
- ELISA, Western blots on treated animal tissue and cell lysates for enzymes, cytokines and other protein targets
- Zymogels for protease activity (MMPs, etc.)
- Biochemical assays for target effectiveness on treated animal tissues
- Whole blood functional assays

BTS Research has also developed low to mid functional HTS fluidics and CCD imaging platforms for a large number of functional cellular assays. The ability to develop assays using these tools speeds the screening process and increases the number of cellular targets that can be tested. Once reagents and protocols have been developed, assays must be validated prior to their use in a screen. All of BTS Research's screening assays are rigorously validated to assure the value of the data generated from our screens.

# INFLAMMATION & DTH MODELS

## Acute TNF-α Production Induced by LPS in Mice……...……2 Weeks

This mouse model is an acute model to evaluate inhibitors that reduce levels of TNF-α induced by a single intra-peritoneal injection of 50 µg of LPS. In this model, mice are treated with the MRC compound 12 hours prior to injection with LPS i.p. 2 hours after the last administration of the MRC compound mice are sacrificed and blood is collected by retro-orbital puncture before any treatment and at time of sacrifice for the measurement of TNF-α levels by ELISA.

## LPS/D-Gal Induced Mortality in Mice and Rats……...…...2 Weeks

This mouse model is an acute inflammation/injury model to evaluate inhibitors that increase survival by reducing the levels of TNF-α induced by a single intra-peritoneal injection of 50 µg of LPS and D-Galactosamine (600 mg/kg). In this model, mice are treated with the test compound 1 hour prior to injection with LPS/D-Gal i.p. Survival of mice is followed for 72 hours following injection with LPS/D-Gal. At 2 hours, blood is collected from all mice by retro-orbital puncture for measurement of TNF-α levels by ELISA.

## In Vivo Analysis of Compounds in the Oxazolone Ear Edema Mouse Model…….....…….....3 Weeks

### Introduction

The contact hypersensitivity (CS) response in mice is a model of clinical allergic contact dermatitis and also a widely employed model for investigating mechanisms of T lymphocyte-mediated inflammation. About 2 h after topical application of Ag to the ear of sensitized mice, there is marked edema due to mast cell degranulation and release of vasoactive mediators such as histamine and serotonin. This is followed by leukocyte migration into the tissues, and a second larger peak of ear swelling occurring about 24 h, after which inflammation spontaneously subsides. There is evidence that local release of

cytokines, including TNF-α, IL-1- α, and IFN- γ, is critical for the optimal generation of the CS reaction

Leukocyte adhesion to endothelium is the first step in their emigration into the tissues; therefore, it is of fundamental importance to the generation of inflammatory responses. Recently, there has been a major increase in our understanding of the mechanisms involved in leukocyte-endothelial cell interactions, with leukocytes undergoing a series of adhesion and activation events consisting of rolling, firm adhesion, and transmigration into the tissues. ICAM-1 and VCAM-1 are members of the Ig superfamily and when expressed by endothelial cells act respectively as ligands for the leukocyte $\beta_2$ and α integrins. Both ICAM-1 and VCAM-1 are thought to be mainly involved in the firm adhesion of leukocytes that are already rolling on endothelial cells, although there is evidence that $\alpha_4$ integrin binding to VCAM-1 may also initiate the interaction of lymphocytes with endothelial cells

The capacity of leukocytes to interact with endothelial cells is in large part determined by the activation of endothelial cells by cytokines such as TNF- α and IL-1- α that leads to the up-regulation or de novo induction of a variety of chemoattractants and surface adhesion molecules including ICAM-1 and VCAM-1.

**Experimental Procedure**

*Contact sensitivity*

Animals will be sensitized 5 days before the experiment by the application of 1% 4-ethoxymethyl-2-phenyl-2-oxazolin-5-one (oxazolone) in acetone/olive oil (4:1) (50 µl) onto the shaved flank of mice. The CS response will be subsequently elicited by applying 1% oxazolone in acetone/olive oil (10 µl) to the right ear, while the left ear will be treated with acetone/olive oil alone. The ear thickness is measured 48 hours after the ear challenge. Ear thickness will be measured using an engineer's micrometer (RS232), and will be expressed as the absolute increase (Δ) in mm over baseline.

*ELISA assays*

Skin biopsies will be obtained from each ear will be homogenized in lysis buffer containing. TNF-α, IL-1α, and INF-γ will be run using commercial ELISA on standardized skin extracts.

## AA-Induced Ear Edema in Mouse……2-3 Weeks

The arachidonic acid (AA)-induced inflammation in mouse ears is a common *in vivo* inflammation model is where arachidonic acid is administered topically to the skin and the subsequent changes in eicosanoid synthesis are examined. AA will significantly increase the eicosanoid synthesis (prostaglandins $E_2$ and $F_{2a}$ and leukotrienes $B_4$ and $C_4/D_4/E_4$) following the topical irritation. This effect peaks at 1 hour and lasts for 3 hours.

**Experimental Procedure:** AA is solubilized in acetone and a 20-µl aliquot and applied to the right ear (10 µl on inner ear and 10 µl on outer ear) of male CD-1 mice (25-30 g).

The right ear of control mice received identical treatment with the acetone vehicle. Drugs can be administered orally or topically (IN order to use topical applications, drug must be soluble in acetone) 1 h before AA administration. The animals are sacrificed 1 h after application of AA. The ears are immediately excised and weighed (in grams). Edema is calculated as the increase in right ear weight of mice treated with AA compared with increase in right ear weight of control mice treated with acetone vehicle.

Ear sections are homogenized in 750 µl of saline, and after centrifugation at 10,000 × *g* for 15 min at 4°C, $PGE_2$, LTs, or LO content in supernatants are determined by immunoassay.

## T Cell Contact Hypersensitivity Skin Migration Model……3-4 Weeks

ROLE OF T CELLS IN THE PATHOLOGY OF CHS

Contact hypersensitivity (CHS) is a T cell-mediated immune response induced by cutaneous application of a reactive hapten. During the sensitization phase, Langerhans cells migrate from epidermis to skin-draining lymph nodes, where they present hapten-MHC complexes to naive T cells. During the elicitation phase that develops after subsequent contact with the hapten, Ag-specific T cells migrate into the site of Ag challenge and release cytokines, thereby initiating the inflammatory response. CHS has long been considered a model of delayed-type hypersensitivity (DTH), which is mediated by CD4+ Th1 cells. Multiple studies suggest, however, that CHS responses are mediated by CD8+ Tc1 cells and down-regulated by CD4+ Th2 cells. The recent study using mice lacking either CD4+ or CD8+ T cells provided evidence that both CD4+ Th1 cells and CD8+ Tc1 cells function as effector cells in CHS responses. To exert effector functions, these cells need to migrate into the site of Ag challenge. The migration of in vitro-generated Th1 cells into the inflamed skin in a CHS model is mediated by P- and E-selectin. In addition, P-selectin glycoprotein ligand-1 (PSGL-1) on Th1 cells has been shown to function as a major P-selectin ligand and one of the E-selectin ligands.

ANIMAL MODEL FOR CHS MIGRATION

P- and E-selectin mediate $CD4^+$ cell migration into the inflamed skin in the murine contact hypersensitivity model.

Mice are sensitized by the application of 100 µl 2% (w/v) oxazolone solution on the shaved abdominal skin on day 0. On day 6, T-cells are harvested from spleens of mice and labeled at a concentration of $1 \times 10^7$/ml. After 2 washes, they are suspended at a concentration of $4 \times 10^6$ and injected into the tail vein of a mouse that had been sensitized 7 days earlier. Mice are sacrificed 3 h after injection and fluorescence in the skin is quantified.

*In-Vivo* Experimentation

**T cell in vivo skin migration mouse model**

All groups will have 10 mice

Conditions to be used:

- Group 1: Negative-No treatment
- Group 2: Positive- Abs to Selectins
- Group 3: Doze 1 of test compound
- Group 4: Doze 2 of test compound
- Group 5: Doze 3 of test compound

Evaluation:

- Quantification of T cell migration in skin

Time to Completion: 3-4 weeks

# ASTHMA & COPD MOUSE MODELS

## Cockroach Asthma Mouse Model

Morbidity due to asthma continues to rise, especially among inner-city children. Recent data indicates that the disproportionate increase in densely populated urban areas appears to be due to allergen exposure. In particular, allergies to cockroach Ag have demonstrated a significant correlation to the rise of adolescent asthma in the more densely crowded inner cities, where large numbers of cockroaches can be found. Although the increase in asthma in inner cities cannot be linked solely to cockroach Ag, as increases in other allergens such as dust house mite have also been detected, 60% of inner city asthmatics have highly elevated IgE levels specific for cockroach Ags. Furthermore, some studies have suggested that the prevalence of sensitivity to cockroach Ags may be comparable with that for mite or cat allergens among acute asthmatics. Such patients are most often found in crowded, lower socioeconomic areas where dwellings are commonly infested with cockroaches. Constant exposure to threshold amounts of specific cockroach allergen establishes a persistent inflammatory response within the airway.

The murine model of cockroach allergen-induced airway hyperreactivity exhibit responses resembling those that have been observed in human asthmatic patients (i.e., airway eosinophilia and airway hyperreactivity. Aerosolized cockroach Ag can be utilized to induce airway inflammation and alter airway physiology in both mice and guinea pigs.

The inflammatory responses induced by cockroach allergen in the murine model are characterized by a significant eosinophilic influx and concurrent airway hyperreactivity. In addition, this model allows a primary challenge and secondary rechallenge stage allergic exacerbations, which elicit different responses in the absence or presence of preexisting eosinophilic inflammation, respectively. Chemokines such as eotaxin, a potent murine eosinophil attractant, has been shown to play a partial role in the primary vs. rechallenge stages of cockroach Ag-induced allergic airway inflammation. Other cytokines such as IL-16 has been suggested to play a complementary role with eotaxin in this model.

## Model Description

### Sensitization and induction of the airway response

Normal Balb/c/J mice are immunized with the cockroach allergen on day 0. In order to localize the response to the lung, the mice will be given an intranasal administration of the of cockroach allergen on day 14. This initial intranasal Ag induces little cellular infiltrate into the lungs of the mice upon histological examination. Mice will be then challenged 3-5 days later (referred to hereafter as primary challenge response) by intratracheal administration of the cockroach allergen. At the time of the intratracheal challenges the allergic mice will receive one of three different doses of inhibitor or a control protein. After 24 hours post-challenge the mice will be examined for airway hyperreactivity and accumulation of leukocyte subsets will be monitored in the BAL and histology sections. Because this model is dependent upon Th2 type immune responses, we will utilize a control treated group using blocking antibodies with known inhibitory function, either anti-IL-4 or anti-IL-13.

### Morphometric analysis of airway and peribronchial eosinophil accumulation

To assess migration of eosinophils into the airway, we will subject the mice to a 1 ml bronchoalveolar lavage (BAL) with PBS containing 25 nM EDTA at various time points postchallenge. The cells were then dispersed using a cytospin and differentially stain with Wright-Giemsa stain. The cell types (mononuclear phagocytes, lymphocytes, neutrophils, and eosinophils) are expressed as a percentage based on 200 total cells counted/sample.

### Quantitation of chemokines and cytokines by ELISA

The levels of eotaxin and IL-5 proteins in BAL will be measured by specific ELISA.

### Measurement of eosinophil peroxidase (EPO)

Cell-free BAL supernatants will be analyzed for EPO as a marker of eosinophil degranulation.

### Measurement of airway hyperreactivity

Airway hyperreactivity is measured using a Buxco mouse plethysmograph, which is specifically designed for the low tidal volumes. Briefly, the mouse tested are anesthetized with sodium pentobarbital and intubated via cannulation of the trachea with an 18-gauge metal tube. The mouse is subsequently ventilated with a Harvard pump ventilator (tidal volume = 0.4 ml, frequency = 120 breaths/min, positive end-expiatory pressure 2.5 to 3.0 cm $H_2O$) and the tail vein is cannulated with a 27-gauge needle for injection of the methacholine challenge. The plethysmograph will be sealed and readings will be monitored by computer. Since the box is a closed system, a change in lung volume is represented by a change in box pressure ($P_{box}$), which was measured by a differential transducer. The system is calibrated with a syringe that delivers a known

volume of 2 ml. A second transducer is used to measure the pressure swings at the opening of the trachea tube ($P_{aw}$), referenced to the body box (i.e., pleural pressure), and to provide a measure of transpulmonary pressure ($P_{tp} = P_{aw} - P_{box}$). The trachea transducer is calibrated at a constant pressure of 20 cm $H_2O$. Resistance is calculated by the Buxco software by dividing the change in pressure ($P_{tp}$) by the change in flow (F) ($\delta P_{tp}/\delta F$; units = cm $H_2O$/ml/s) at two time points from the volume curve, based upon a percentage of the inspiratory volume. Once the mouse is hooked up to the box it will be ventilated for 5 min prior to acquiring readings and the peak airway resistance is recorded as a measure of airway hyperreactivity.

**Cockroach Asthma Mouse Model…….……4-6 Weeks**

Conditions to be used:

1. A standard of ten mice are used per condition for a total of 60 mice for 6 conditions:
    a. Negative Control: No treatment-10 Mice
    b. Positive Control: 10 Mice
    c. Positive Control: Anti-IL-14 or IL-13 mAb i.p.- 10 Mice
    d. Dose 1 of compound-10 Mice
    e. Dose 2 of compound–10 Mice
    f. Dose 3 of compound–10 Mice

# OVA Asthma Mouse Model

## Mice

Female BALB/c mice at 6–8 wk of age are used.

## Allergen sensitization/challenge protocol

OVA (500 µg/ml) in PBS is mixed with equal volumes of 10% (w/v) aluminum potassium sulfate in distilled water and incubated for 60 min at room temperature after adjustment to pH 6.5 using 10 N NaOH. After centrifugation at 750 x *g* for 5 min, the OVA/alum pellet is resuspended to the original volume in distilled water. Mice receive an i.p. injection of 100 µg OVA (0.2 ml of 500 µg/ml in normal saline) complexed with alum on day 0. Mice are anesthetized by i.p. injection of a 0.2-ml mixture of ketamine and xylazine (0.44 and 6.3 mg/ml, respectively) in normal saline and are placed on a board in the supine position. Two hundred fifty micrograms (100 µl of a 2.5 mg/ml) of OVA (on day 8) and 125 µg (50 µl of 2.5 mg/ml) OVA (on days 15, 18, and 21) are placed on the back of the tongue of each animal. The deposition pattern of the OVA by this i.t. delivery is examined using toluidine blue dye. OVA (2.5 mg/ml) is mixed in toluidine blue, and 100 µl was administered by i.t. delivery. The majority of the toluidine blue dye staining is seen in the lumen and interstitium of the tracheal wall, with the remainder in the lumen and interstitium of the small airways. Toluidine blue dye staining is not detected in the esophagus or stomach. Control mice receive i.p. saline with alum on day 0 and i.t. saline on days 8, 15, 18, and 21.

## Drug treatment

Test substance is given according to client specification.

## Pulmonary function testing

In vivo airway responsiveness to methacholine is measured 24 h after the last OVA challenge in conscious, freely moving, spontaneously breathing mice using whole body plethysmography. Mice are challenged with aerosolized saline or increasing doses of methacholine (5 and 20 mg/ml) generated by an ultrasonic nebulizer for 2 min. The degree of bronchoconstriction is expressed as enhanced pause ($P_{enh}$), a calculated dimensionless value, which correlates with the measurement of airway resistance, impedance, and intrapleural pressure in the same mouse. $P_{enh}$ readings are taken and averaged for 4 min after each nebulization challenge. $P_{enh}$ is calculated as follows: $P_{enh} = [(T_e/T_r - 1) \times (PEF/PIF)]$, where $T_e$ is expiration time, $T_r$ is relaxation time, PEF is peak expiratory flow, and PIF is peak inspiratory flow x 0.67 coefficient. The time for the box pressure to change from a maximum to a user-defined percentage of the maximum represents the relaxation time. The $T_r$ measurement begins at the maximum box pressure and ends at 40%.

**Bronchoalveolar lavage**

After measurement of airway hyper-reactivity, the mice undergo exsanguination by cardiac puncture, and then BAL iss collected (0.4 ml saline, three times) from the right lung after tying off the left lung at the mainstem bronchus. Total BAL fluid cells are counted from a 0.05-ml aliquot, and the remaining fluid is centrifuged at 200 x *g* for 10 min at 4°C. Cell pellets are resuspended in saline containing 10% BSA with smears made on glass slides.

Eosinophils are stained for 5 min with 0.05% aqueous eosin and 5% acetone in distilled water, rinsed with distilled water, and counterstained with 0.07% methylene blue.

**Lung histopathology**

After BAL, the trachea and upper and lower lobes of the left lung are removed and fixed for 24 h in 10% neutral buffered formalin solution. The tissues are embedded in paraffin and cut into 5-µm sections. The tissue sections are stained with Discombe's solution to identify eosinophils, with H&E to identify neutrophils/other inflammatory cells and edema, and with Alcian Blue, pH 2.5, and Nuclear Fast Red counterstaining to identify airway goblet cells and mucus. The degree of airway inflammatory cell infiltration (0–4+), the number of eosinophils and neutrophils per unit airway area (2200 $\mu m^2$; goblet cell number (percentage of airway cells), mucus occlusion of airway diameter (0–4+), and airway edema (0–4+) were determined by morphometry.

**Cytokine assays**

BAL fluid levels of IL-4 (≥2 pg/ml), IL-13 (≥1.5 pg/ml), and eotaxin (≥3 pg/ml) are determined by commercial ELISA kits.

**OVA Asthma Mouse Model…….……...……4-6 Weeks**

Conditions to be used:

2. A standard of ten mice are used per condition for a total of 60 mice for 6 conditions:
    a. Negative Control: No treatment-10 Mice
    b. Positive Control: 10 Mice
    c. Positive Control: Anti-IL-14 or IL-13 mAb i.p.- 10 Mice
    d. Dose 1 of compound-10 Mice
    e. Dose 2 of compound–10 Mice
    f. Dose 3 of compound–10 Mice

## Mechanical Tracheal Ring Assay

This assay is performed on freshly obtained rabbit trachea. In this assays, rabbits are killed by an overdose of pentobarbital sodium, and their tracheae are immediately excised and incubated in a physiological saline solution [containing (in mM) 118 NaCl, 4.5 KCl, 2.5 $CaCl_2$, 1.2 $MgSO_4$, 1.2 $KH_2PO_4$, 25.5 $NaHCO_3$, and 5.6 glucose] bubbled with 95% $O_2$-5% $CO_2$. The tracheae are dissected from surrounding tissues and cut into ~3-mm rings. Only those rings from the lower end of the trachea are used to measure the mechanical responses. The tracheal rings are mounted on hooks, connected to force transducers, and incubated in physiological saline solution bubbled with 95% $O_2$-5% $CO_2$ in 25-ml organ baths at 37°C. The passive tension is set at 1 g, and the tissue is equilibrated for 60 min. The isometric force of the tracheal rings in response to carbachol is recorded. The magnitude of relaxation induced by formamidoxime ($HC(NH_2)$==NOH) is measured on rings that were preconstricted with $10^{-6}$ M carbachol and calculated as the percent decrease in the isometric force developed with carbachol. The effects of test articles on formamidoxime-induced relaxation of tracheal rings is also recorded.

## PPE-Induced COPD in Mice

Chronic obstructive pulmonary disease (COPD) is one of the commonest reasons for ill health worldwide. Intrapulmonary challenge with injurious proteins, chemicals, particulates, and other compounds into lungs of animals has been used to cause emphysema directly. Compounds have also been administered that inhibit protein function (loss of function models), resulting in airspace enlargement.

A single intrapulmonary challenge with proteinases including porcine pancreatic elastase (PPE), papain, and human neutrophil elastase causes panacinar emphysema. Their effectiveness was directly related to their elastolytic activity, while instillation of bacterial collagenases did not cause emphysema. PPE mediated emphysema is accompanied by secretory cell metaplasia and abnormalities of pulmonary function, hypoxaemia, and right ventricular hypertrophy that are characteristic of human COPD. Following an intratracheal bolus of PPE, there is an initial loss of elastin and collagen. Over time, elastin and glycosaminoglycans return to normal and collagen is enhanced, yet intraparenchymal extracellular matrix (ECM) remains diminished and distorted and the architecture of the lung is grossly and permanently abnormal. Airspace enlargement develops immediately after elastolytic injury, followed by inflammation. The subsequent progression of emphysema over the next few months is probably caused by the destructive effect of host inflammatory proteinases.

### Mice

Female BALB/c mice at 6–8 wk of age are used.

### Drug treatment

Test substance is given according to client specification.

### Pulmonary function testing

In vivo airway responsiveness to methacholine is measured starting of day 7 after the PPE chanllenge and weekly thereafter until day 21 in conscious, freely moving, spontaneously breathing mice using whole body plethysmography. Mice are challenged with aerosolized saline or increasing doses of methacholine (5 and 20 mg/ml) generated by an ultrasonic nebulizer for 2 min. The degree of bronchoconstriction is expressed as enhanced pause ($P_{enh}$), a calculated dimensionless value, which correlates with the measurement of airway resistance, impedance, and intrapleural pressure in the same mouse. $P_{enh}$ readings are taken and averaged for 4 min after each nebulization challenge. $P_{enh}$ is calculated as follows: $P_{enh} = [(T_e/T_r - 1) \times (PEF/PIF)]$, where $T_e$ is expiration time, $T_r$ is relaxation time, PEF is peak expiratory flow, and PIF is peak inspiratory flow x 0.67 coefficient. The time for the box pressure to change from a maximum to a user-defined percentage of the maximum represents the relaxation time. The $T_r$ measurement begins at the maximum box pressure and ends at 40%.

**Bronchoalveolar lavage**

After measurement of airway hyper-reactivity, the mice undergo exsanguination by cardiac puncture, and then BAL is collected (0.4 ml saline, three times) from the right lung after tying off the left lung at the mainstem bronchus. Total BAL fluid cells are counted from a 0.05-ml aliquot, and the remaining fluid is centrifuged at 200 x *g* for 10 min at 4°C. Cell pellets are resuspended in saline containing 10% BSA with smears made on glass slides.

Neutrophils and macrophages are stained and counted

**Measurement of Myeloperoxidase (MPO)**

Cell-free BAL supernatants can be analyzed for MPO as a marker of neutrophil and macrophage degranulation.

**Lung histopathology**

After BAL, the trachea and upper and lower lobes of the left lung are removed and fixed for 24 h in 10% neutral buffered formalin solution. The tissues are embedded in paraffin and cut into 5-μm sections. The tissue sections are stained with Discombe's solution to identify eosinophils, with H&E to identify neutrophils/other inflammatory cells and edema, and with Alcian Blue, pH 2.5, and Nuclear Fast Red counterstaining to identify airway goblet cells and mucus. The degree of airway inflammatory cell infiltration (0–4+), the number of neutrophils and macrophage per unit airway area (2200 $\mu m^2$; goblet cell number (percentage of airway cells), mucus occlusion of airway diameter (0–4+), and airway edema (0–4+) were determined by morphometry.

**Cytokine assays**

BAL fluid levels of Gro-α and MCP-1 mouse equivalents (≥2 pg/ml) are determined by commercial ELISA kits.

# COLLAGEN-INDUCED ARTHRITIS (CIA)

**Collagen-induced arthritis (CIA)……14-18 Weeks**

Collagen-induced arthritis (CIA) in the mouse is induced by immunization of susceptible mice strains with native type II collagen. Macroscopically evident arthritis occurs between days 28-35 after immunization and persists for several months until the joints ankylose. Mice are followed for a subsequent period of 60 days. CIA shares several histopathologic features with RA including mononuclear cell infiltration and synovial cell hyperplasia resulting in pannus formation with bone and cartilage destruction. In both RA and CIA, disease susceptibility is restricted by MHC class II alleles and autoreactive T cells are prominent in the joint with restriction in Vb T cell receptor usage. Because of these similarities, CIA is a widely used experimental model for RA.

Conditions to be used:

1. A standard of ten mice are used per condition:
    a. Negative Control: No treatment-10 Mice
    b. Positive Control: CsA, P38 inhibitors, Anti-TNF-a/IL-1 at highest dose- 10 Mice
    c. Compound at Dose level 1- 10 Mice
    d. Compound at Dose level 2- 10 Mice
    e. Compound at Dose level 3- 10 Mice

The following are the scores used in the evaluation of potential arthritis drugs in the CIA arthritis model:

- **Swelling Score:** Swelling is determined by Ankle Width Measurement (AWM)
- **Histopathological Score:** Histopathological score is the combination of the following four scores
    - Subsynaovial Inflammation (characterized by mononuclear cell resembling nodule formation)
    - Pannus Formation
    - Bone Erosion
    - Synovial Hyperplasia
- **Radiological Score:** Radiological score is determined by X-Ray of the ankle of mice taken at the beginning of the model and at the sacrifice of the animals
- **Cytokine Analysis Score:** This done by measuring the levels of Tumor Necrosis Factor (TNF-α), Interleukin-1 (IL-1), JE/CCLE (mouse Monococyte Chemotactic Protein-1), and Interleukin-8 (IL-8) at Weeks 0, 4, 8, 12

# EXPERIMENTAL AUTOIMMUNE ENCEPHALOMYELITIS (EAE) MOUSE MODELS

## Active EAE-MOG-Induced and Relapse PLP-Induced Mouse Model

## INTRODUCTION

Multiple sclerosis (MS), is an inflammatory disease in the CNS characterized by demyelination and axon damage leading to severe neurological dysfunction. Leukocytes are present in the CNS lesion, and $CD4^+$ T cells and macrophages are considered the primary cell types in the initiation stage of the disease process. The triggering event for the pathogenesis in MS is not known, but both genetic and environmental factors contribute to disease. Association studies have demonstrated that susceptibility is associated with genes in the MHC. A number of additional, potentially important genetic regions have been suggested, but to date no major susceptibility gene has been found.

Animal models, resembling human disease, are important tools for studying complex genetic traits, and recent comparable analysis of the mouse and human genomes has highlighted the striking similarity in their genes and genetic organization. Experimental autoimmune encephalomyelitis (EAE), a model for MS, is induced in genetically susceptible rodents by immunization with myelin proteins or peptides. The myelin basic protein (MBP) or $MOG_{35-55}$ peptides were demonstrated to bind to the MHC class II molecule of the HLA-DR2 haplotype, which is strongly associated with susceptibility to MS.

**EAE……7 Weeks**

### EAE Disease Induction with MOG and Clinical Scoring:

EAE induction will be performed according to the following protocol. In brief, 300 µg of myelin oligodendrocyte glycoprotein $(MOG)_{35–151}$ peptide will be dissolved in 100 µl of PBS and emulsified in an equal volume of CFA containing 5 mg/ml of *Mycobacterium tuberculosis* H37 RA. The emulsion (200 µl) will be injected subcutaneously into the flank on days 0 and 7. Pertussis toxin, 500 ng in 500 µl of PBS (List Biological Labs.), will be administered intravenously into each tail vein on days 0 and 2. Mice will be

scored daily according to the following clinical scoring system: 0, no clinical disease; 1, tail flaccidity; 2, hind limb weakness; 3, hind limb paralysis; 4, forelimb paralysis or loss of ability to right from supine; 5, death.

**EAE Disease Induction with PLP with PTX and Clinical Scoring:**

Female SJL/J mice (6-9 weeks old) will be injected with 100ug proteolipid protein (PLP) 139−151 (HSLGKWLGHPDKF) peptide. 100ug of the PLP Peptide will be dissolved at 5 mg/ml in distilled water and emulsified with an equal volume of Freund's adjuvant containing 5 mg/ml of H37Ra M. tuberculosis (Difco). On the day of initiation of EAE, referred to as day 1 of the experiment, mice will receive a single injection of 100 ul of emulsion subcutaneously in a skin fold at the back of the neck. On day 1, they will also receive 250 ng of pertussis toxin (List Biological Labs, Campbell, USA) from a solution of 50 ug/ml in 0.01 M sodium phosphate buffer pH7.0 with 0.9% NaCl IP. This injection was repeated on day 3. Mice will be scored daily according to the following clinical scoring system: 0, no clinical disease; 1, tail flaccidity; 2, hind limb weakness; 3, hind limb paralysis; 4, forelimb paralysis or loss of ability to right from supine; 5, death.

**EAE Disease Induction with PLP no PTX and Clinical Scoring:**

Female SJL/J mice (6-9 weeks old) will be injected with 100ug proteolipid protein (PLP) 139−151 (HSLGKWLGHPDKF) peptide. 100ug of the PLP Peptide will be dissolved at 5 mg/ml in distilled water and emulsified with an equal volume of Freund's adjuvant containing 5 mg/ml of H37Ra M. tuberculosis (Difco). On the day of initiation of EAE, referred to as day 1 of the experiment, mice will receive a single injection of 100 ul of emulsion subcutaneously in a skin fold at the back of the neck. Mice will be scored daily according to the following clinical scoring system: 0, no clinical disease; 1, tail flaccidity; 2, hind limb weakness; 3, hind limb paralysis; 4, forelimb paralysis or loss of ability to right from supine; 5, death.

Conditions to be used:

1. A standard of ten mice are used per condition for a total of 100 mice for 5 conditions(groups):
    a. Negative Control: No treatment-20 Mice
    b. Positive Control: Estrogen- 20 Mice
    c. Compound #1 Dose 1- 20 Mice
    d. Compound #1 Dose 2- 20 Mice
    e. Compound #1 Dose 3- 20 Mice

The model will be stopped at 30 days after induction where most of the animals have reached a clinical score of at least 3-3.5.

## T cell proliferation/inhibition assay……..4 Weeks

APC (irradiated syngeneic spleen cells, $2 \times 10^5$/well) will be pre-incubated in 48-well flat-bottom microtiter plates with an optimal dose (20µg/ml) of $pMOG_{35–151}$. After 1 h, enriched T cells ($4 \times 10^4$/well), prepared from spleens by nylon wool adhesion, will be seeded and further incubated for 48–72-120 h. The cultures will be then pulsed with 1.0 µCi [$^3$H]thymidine/well for 6 h and harvested, and the incorporated isotope will be quantitated by liquid scintillation.

## Cytokine Analysis During T cell proliferation/inhibition assay……2 weeks

Before µCi [$^3$H]thymidine pulsing, 300ul of supernatant will be transferred and evaluated for analysis of the following cytokines:

- At 48h: IL-2 and IL-12
- At 72h: IFN, TNF, and TGF
- At 120h: IL-4and IL-10

## Chronic Relapse/Remission EAE (CREAE) Mouse Model

**EAE Disease Induction and Clinical Scoring:**

CREAE is induced in 6- to 8-week-old female Biozzi ABH mice by injection of 1mg of lyophilized, autologous whole spinal cord homogenate reconstituted in PBS and mixed with CFA supplemented with 320ug/ml of *Mycobacterium Tuberculosis* H37 RA and 40 ug/ml of *Mycobacterium Butyricum* on day 0 and 7, and with pertussis toxin intraperitoneally on day 0, 1, 7 and 8. Animals with complete hindlimb paralysis are examined during the initial acute paralytic attack on day 18 after immunization and the first clinical relapse on days 37 to 42 after immunization. Animals are also examined during the first clinical remission on days 27 to 28 after immunization in which animals exhibited only minimal tail paresis and chronically affected remission animals after three relapses on days 80 to 100, in which animals had residual hindlimb paresis.

Conditions to be used:

2. A standard of ten mice are used per condition for a total of 100 mice for 5 conditions(groups):
    a. Negative Control: No treatment-20 Mice
    b. Positive Control: Estrogen- 20 Mice
    c. Compound #1 Dose 1- 20 Mice
    d. Compound #1 Dose 2- 20 Mice
    e. Compound #1 Dose 3- 20 Mice

## RAG-/-/TR- Spontaneous EAE Model

# INTRODUCTION

Experimental allergic or autoimmune encephalomyelitis (EAE), the prototypical rodent model of human multiple sclerosis (MS), is an autoimmune disease characterized by inflammation in the central nervous system (CNS). Like the human disease, EAE is associated with an early breach of the blood–brain barrier, focal perivascular mononuclear cell infiltrates, and demyelination leading to paralysis of the extremities. The adoptive transfer of myelin-specific $CD4^+$ T cells to naive animals passively confers EAE, demonstrating that this cell type is critical in the disease process. However, it is unclear whether these T cells directly damage the myelin sheath or if they activate other cells for this function. The underlying cause of increased vascular permeability that facilitates the entry of T cells into the CNS is also unknown.

Spontaneous experimental autoimmune encephalomyelitis (EAE) develops in 100% of mice harboring a monoclonal myelin basic protein (MBP)-specific CD4+ alphabeta T-cell repertoire. Monoclonality of the alphabeta T-cell repertoire can be achieved by crossing MBP-specific T-cell receptor (TCR) transgenic mice with either RAG-/- mice or TCR alpha-/-/TCR beta-/- double knockout mice.

In this model, mice start developing EAE after 50 days of their birth and diseases penetration is full after 100 days of birth as shown in the figure below.

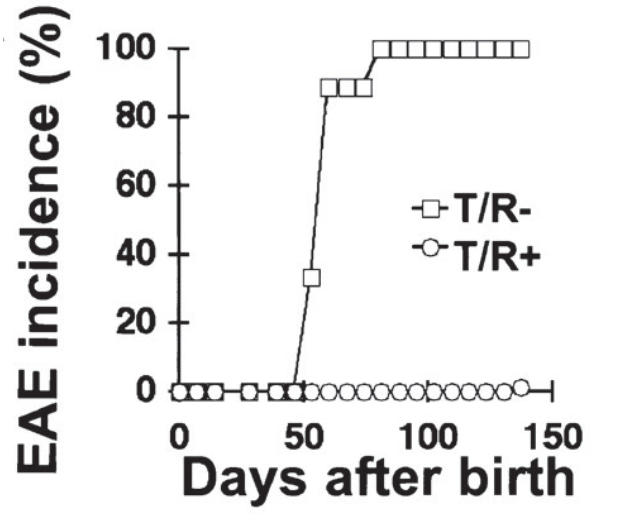

**EAE…….5 Weeks**

**EAE Clinical Scoring**

Mice will be scored daily according to the following clinical scoring system: 0, no clinical disease; 1, tail flaccidity; 2, hind limb weakness; 3, hind limb paralysis; 4, forelimb paralysis or loss of ability to right from supine; 5, death.

Conditions to be used:

3. A standard of ten mice are used per condition for a total of 40 mice for 5 conditions(groups):
    a. Negative Control: No treatment-10 Mice
    b. Positive Control: Estrogen- 10 Mice
    c. Compound #1 Dose 1- 10 Mice
    d. Compound #1 Dose 2- 10 Mice

Compounds will be administered to mice at 40 days after birth and followed for another 60 days.

The model will be stopped at 100 days after birth where most of the animals have reached a clinical score of at least 3-3.5.

**Cytokine Analysis at 100 days ……..……9 weeks**

Blood will be collected, and serum will be evaluated for analysis of the following cytokines:

- IL-2 and IL-12
- IFN-g, TNF-a, and TGFb-1
- IL-4 and IL-10

# INFLAMMATION DISEASE MODELS (GI)

Phone: (858) 605-5882
Toll Free: (866) 599-3019
Fax: (858) 605-5916
P.O. Box 910418, San Diego, CA 92191
www.btsresearch.com

The IBDs are chronic, idiopathic disorders primarily of the ileum and/or colon that are characterized by abdominal pain, severe diarrhea, rectal bleeding, and weight loss. Involved regions of the bowel often exhibit an intense infiltration of leukocytes (including granulocytes and lymphocytes), crypt cell hyperplasia, interstitial edema, and mucosal ulcerations.

TNBS1 or DSS-induced experimental colitis in mice (i.e., TNBS1 colitis induced by the haptenating agent, 2,4,6-trinitrobenzene sulfonic acid) has proven to be an exceptionally useful model of certain forms of human inflammatory bowel disease. For example, the study of this model has led to the recognition that an IL-12-driven, Th1 T cell-mediated inflammation of the colon is not only prevented by the systemic administration of anti-IL-12 antibody, but can also be treated by such administration. This observation has provided the theoretical justification for the use of inhibitors of IL-12, including anti-IL-12 itself, in the treatment of Crohn's disease, an inflammation also dominated by a Th1 T cell response. Studies of the TNBS or the DSS colitis model have also shown that administration of TNBS or DSS per rectum and per os have very different effects; rectal administration results in severe colitis whereas oral administration leads to the induction of suppressor T cells producing TGF-β and the inhibition of colitis caused by TNBS or DSS given simultaneously by the rectal route. These findings in concert with similar findings in other models establish that mucosal inflammation and/or its prevention depend at least in part on a balance between proinflammatory Th1 T cell responses and antiinflammatory TGF-β responses.

**DSS-induced Colitis**

C57BL/6J-664 (wild-type [WT]) mice at 10–12 wk of age will be used. All experimental procedures involving the use of animals are reviewed and approved by the Institutional Animal Care and Use Committee of LSU Health Sciences Center

Colitis is induced by feeding mice 3% DSS (mol wt, 40,000) dissolved in drinking water (Millipore water) for 7 d. In pilot experiments, WT mice were given 3 or 5% (wt/vol) DSS in drinking water for 7 d. Since the mortality rate of mice receiving 5% DSS was nearly one-third, 3% DSS treatment for 7 d (0% mortality) was chosen as an optimal dose for detailed analyses. In control mice, normal drinking water was replaced by millipore water.

**Assessment of Inflammation in DSS-treated Mice**

Daily clinical assessment of DSS-treated animals included measurement of drinking volume and body weight, evaluation of stool consistency, and the presence of blood in the stools by a guaiac paper test (ColoScreen®; Helena Laboratories). A previously

validated clinical disease activity index (DAI; reference ranging from 0 to 4 was calculated using the following parameters: stool consistency; presence or absence of fecal blood; and weight loss. Mice are killed at day 7, blood will be collected by cardiac puncture, and spleens will be weighed. Colons will be removed; length and weight will be measured

**Histopathology**

Histological examination will be performed on three samples of distal colon of each animal, which will be fixed in Zamboni's solution before embedding in JB-4 (Polysciences) and staining with hematoxylin and eosin. All histological quantitation is performed in a blinded fashion using the following scoring system: 1/severity of inflammation, 2/depth of injury, and 3/crypt damage. The score of each parameter will be multiplied by a factor reflecting the percentage of tissue involvement and added to a sum. The maximum possible score is 40.

**Serum TNF Measurements**

On day 7 of the protocol, blood ill be collected from control and DSS-treated mice for determination of serum TNF- α levels by ELISA for murine TNF-α.

This quotation is based on testing one compound at three doses according to the following protocol:

**Group 1: Control-No DSS treatment**
**Group 2: DSS Treatment**
**Group 3: DSS plus Inhibitor (highest dose)**
**Group 4: DSS plus compound at dose 1 (p.o or i.r)**
**Group 5: DSS plus compound at dose 1 (p.o or i.r)**
**Group 6: DSS plus compound at dose 1 (p.o or i.r)**

## OXAZOLONE-INDUCED COLITIS IN MICE (TH2 TYPE DISEASE MODEL)

While, as indicated above, TNBS and DSS have proven as useful agents in the induction of experimental colitis, their effects on the colon may be limited by the range of T cell responses it is capable of inducing. In this regard, previous studies imply that haptenating agents differ somewhat with respect to the cell populations they address and thus differ somewhat in the type of immune responses they induce. Is was found that oxazolone elicited a very different colitis than that obtained with TNBS or DSS administration in that it induced a colitis involving only the distal half of the colon and had histologic features resembling ulcerative colitis (UC) rather than Crohn's disease. In addition, oxazolone colitis is IL-4- driven rather than IL-12-driven, is prevented by the administration of anti-IL-4, and is exacerbated by the administration of anti-IL-12.
Rectal administration of oxazolone, in contrast to TNBS or DSS, induces a TGF-β response which plays an important role in limiting the inflammation both in extent and in time.

**Oxazolone-induced Colitis**

Pathogen-free, 5-6-wk-old male SJL/J mice are used in this model. For induction of colitis, mice will be first lightly anesthetized with metofane (methoxyflurane) and then 6 mg of the haptenating agent, oxazolone (4-ethoxymethylene-2-phenyl-2-oxazolin-5-one), will be administered per rectum via a 3.5 F catheter equipped with a 1-ml syringe. The catheter will be inserted so that the tip will be 4 cm proximal to the anal verge and the oxazolone will be injected with a total volume of 150 µl of a 1:1 H2O/ethanol mixture (50% ethanol). To ensure distribution of the oxazolone within the entire colon and cecum, mice are held in a vertical position for 30 s after the injection.

**Histopathology**

Tissues obtained at indicated time points were fixed in 10% buffered formalin phosphate and then embedded in paraffin, cut into sections, and then stained with hematoxylin and eosin. Stained sections are scored according to the following criteria:

1. Elongation and/or distortion of crypts
2. Crypt abscesses
3. Reduction in goblet cell number
4. Frank ulceration
5. Edema formation.

**TGF-β Measurements from ex vivo Spleens**

Spleen T cells from mice are cultured for evaluation of TGF-β production in serum-free media supplemented with 1% nutridoma-SP by ELISA.

This quotation is based on testing one compound at three doses according to the following protocol:

**Group 1: Control-No DSS treatment**
**Group 2: DSS Treatment**
**Group 3: DSS plus Inhibitor (highest dose)**
**Group 4: DSS plus compound at dose 1 (p.o or i.r)**
**Group 5: DSS plus compound at dose 1 (p.o or i.r)**
**Group 6: DSS plus compound at dose 1 (p.o or i.r)**

## INFLAMMATORY BOWEL DISEASE (IBD) INDUCED IN SCID MICE BY THE ADOPTIVE TRANSFER OF LOW NUMBERS OF THE FOLLOWING PURIFIED BALB/C $CD4^+$ T CELL

$CD45RB^{high}$ $CD4^+$ T cells from normal rats have the potential to induce autoimmune diseases in congenic, immunodeficient hosts. $CD45RB^{high}$ $CD4^+$ T cells from healthy animals thus seem to express an autoaggressive potential that can be revealed in vivo.
Adoptive transfer into SCID host of comparable numbers of $CD4^+$ T cells can be used to assess the beneficial effects of drugs or antibodies to the T-cell induced colitis n these mice.
Small $CD45RB^{high}$ $CD4^+$ T lymphocytes and activated $CD4^+$ T blasts induce early (6–12 wk post transfer) and severe disease, while small resting and unfractionated CD41 T cells or CD45RBlow T lymphocytes induced a late-onset disease 12–16 wk post transfer.

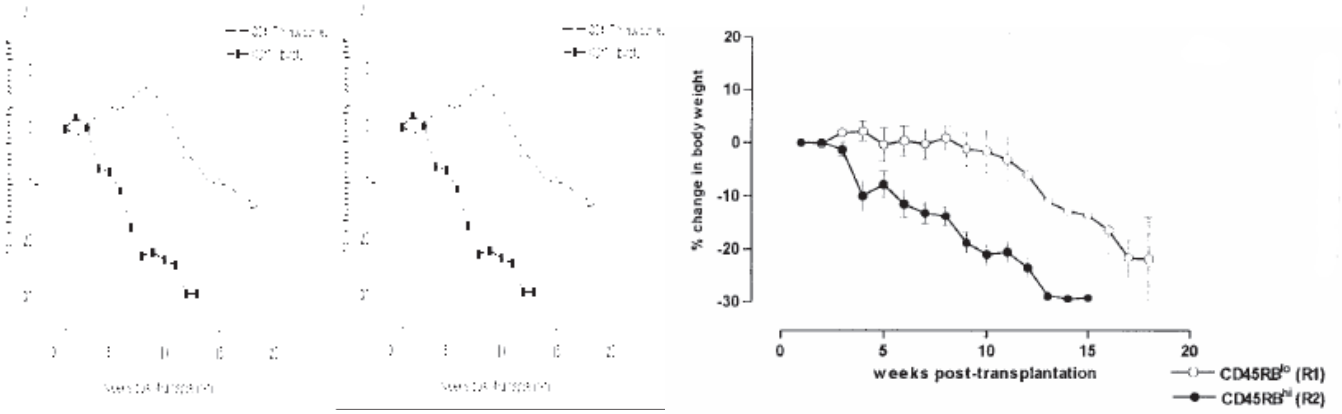


$CD45RB^{high}$ $CD4^+$ T cell from BALB/cJ mice are transplanted i.p. into SCID mice at 4–6 wk of age.
Transplanted mice are monitored for:

1. Weight loss
2. Rectal prolapse
3. Rectal bleeding
4. Diarrhea

Mice are sacrificed for histological and/or cytological examinations when they exhibited two or more of the following signs of disease:

1. A loss of .15% of their adult body weight (compared with a group of nontransplanted SCID mice)
2. The development of a large (.3 mm) rectal prolapse
3. or extensive diarrhea or bloody stools

**Role of CCR9 in IBD and Colitis**

CCR9, previously known as GPR-9-6, is the receptor for the chemokine CCL25/TECK (thymus expressed chemokine). CCR9 is expressed as two isoforms, CCR9A and CCR9B with the "A" form containing 12 additional amino acids at its N-terminus. CCR9 receptors are expressed on both mature and immature thymocytes as well as low level expression on some peripheral T cells and T cells lines such as MOLT-4, MOLT-13 and SUPT-T1. B cells, $CD4^+$ and $CD8^+$ memory T cells have also demonstrated low level expression of CCR9. There is some evidence that the CCR9A isoform may be expressed at 10-fold higher levels than CCRB in thymocytes and peripheral lymphoid cells. Of particular interest is the fact that CCR9 expression can be used as a tool to identify gut homing $\alpha_4 b_7^+$ memory T cells from $CCR9^-$ $CLA^+$ (cutaneous lymphocyte-associated antigen) memory T cells that home to non-gut lymphoid organs. Other peripheral blood cells, such as NK cells, monocytes, neutrophils, basophils, eosinophils and dendritic cells, all appear to lack expression of CCR9.

Chemokine receptors are key determinants of leucocyte trafficking. Chemokine receptor CCR9 and its chemokine ligand CCL25 (TECK) mediate lymphocyte homing to the healthy small intestine and have been shown to be overexpressed in colitis or IBD diseases states.

## Acute Gastric Irritation in mice or rats (4hrs)

- Prevention of gastric lesions induced by HCl (4hrs) in rats or mice performed in 24 hour fasted rats or mice.
- Appropriate dose of test compound administered and followed 30-60 minutes later with lesion inducing agent.
- Animals are sacrificed 3 hours later and stomach examined for presence of mucosal lesions.
- 10 animals per dose group
- The lesion index was determined as the sum of erosion length per mouse

## Acute Gastric Irritation in mice or rats (24hrs)

- Prevention of gastric lesions induced by alcohol (24hrs), aspirin (24hrs), or NSAIDs (24hrs) in rats or mice performed in 24 hour fasted rats or mice.
- Appropriate dose of test compound administered and followed 30-60 minutes later with lesion inducing agent.
- Animals are sacrificed 3 hours later and stomach examined for presence of mucosal lesions.
- 10 animals per dose group
- Ethanol induced lesion is assessed and scored for severity according to:
  - (0): Absence of lesion
  - (1): Superficial 1–5 hemorrhagic points
  - (2): Superficial 6–10 hemorrhagic points
  - (3): Submucosal hemorrhagic lesions with small erosions
  - (4): Severe hemorrhagic lesion and some invasive lesions.

## Prevention of NSAID Induced Intestinal Lesions

- Prevention of gastric lesions induced by alcohol, aspirin, or NSAIDs in the rat performed in 24 hour fasted rats.
- Appropriate dose of test compound administered and followed 30-60 minutes later with lesion inducing agent.

# INFLAMMATION DISEASE MODELS (GI)

## Acute Gastric Irritation in mice or rats (4hrs)

- Prevention of gastric lesions induced by HCl (4hrs) in rats or mice performed in 24 hour fasted rats or mice.
- Appropriate dose of test compound administered and followed 30-60 minutes later with lesion inducing agent.
- Animals are sacrificed 3 hours later and stomach examined for presence of mucosal lesions.
- 10 animals per dose group
- The lesion index was determined as the sum of erosion length per mouse

## Acute Gastric Irritation in mice or rats (24hrs)

- Prevention of gastric lesions induced by alcohol (24hrs), aspirin (24hrs), or NSAIDs (24hrs) in rats or mice performed in 24 hour fasted rats or mice.
- Appropriate dose of test compound administered and followed 30-60 minutes later with lesion inducing agent.
- Animals are sacrificed 3 hours later and stomach examined for presence of mucosal lesions.
- 10 animals per dose group
- Ethanol induced lesion is assessed and scored for severity according to:
  - (0): Absence of lesion
  - (1): Superficial 1–5 hemorrhagic points
  - (2): Superficial 6–10 hemorrhagic points
  - (3): Submucosal hemorrhagic lesions with small erosions
  - (4): Severe hemorrhagic lesion and some invasive lesions.

## Prevention of NSAID Induced Intestinal Lesions

- Prevention of gastric lesions induced by alcohol, aspirin, or NSAIDs in the rat performed in 24 hour fasted rats.
- Appropriate dose of test compound administered and followed 30-60 minutes later with lesion inducing agent.

- Rats sacrificed 3 hours later and stomach examined for presence of mucosal lesions.
- Prevention of perforating small intestine ulcers induced by indomethacin in the rat performed in fed rats.
- Test agent administered daily for three days. Indomethacin administered 1 hour after first dose of test agent.
- Rat sacrificed on third day. Rats receiving indomethacin alone will show significant incidence of small intestinal lesions.

# SYSTEMIC LUPUS ERYTHEMATOSUS (SLE) MOUSE MODELS

All of the known SLE animal models are spontaneously occurring autoimmune diseases such as the systemic lupus erythematosus (SLE)-like syndrome in Murphy Roth Lab lymphoproliferative (MRL/lpr mice and in the offspring between New Zealand black/New Zealand white mice (NZB/NZW F1 hybrid [B/W]. The MRL/lpr strain of mice develops a massive lymphoproliferative disease characterized by arthritis, glomerulonephritis, vasculitis, and anti-double-stranded (anti-ds) DNA antibody. These mice have a single gene defect that prevents high level expression of Fas, a protein that signals for apoptosis. Normal mice express high levels of the Fas protein on CD4/CD8 double-positive thymocytes, inducing apoptosis of potentially autoreactive T-cell clones. T-cells normally upregulate Fas-surface protein when activated, which serves to control a lymphoproliferative response by inducing cell death. In MRL/lpr mice, autoimmunity results from a lack of normal lymphocyte programmed cell death. Transplantation of hematopoietic stem cells from MRL/lpr mice into an unaffected strain of mice results in the MRL/lpr phenotype and early death. The NZB mouse develops spontaneous hemolytic anemia and a high titer of antierythrocyte antibodies. When bred with the phenotypically normal NZW mouse, the offspring (F1 hybrid, B/W) develop a fatal immune glomerulonephritis and a high titer of anti-ds DNA antibody. Although hemolysis may occur, it is not prominent. The genetic defect in B/W mice is unknown, but transplantation of lymphocyte-depleted marrow into a normal mouse from another strain causes fatal immune glomerulonephritis.

**A list of available mouse lupus models is listed in the following table. Please inquire for pricing.**

| Mouse Strain | MHC Haplotype | Major Clinical Features | Survival Time of 50% of Animals in Typical Groups | Sexes Affected | Major Immunological Features |
|---|---|---|---|---|---|
| New Zealand Black (NZB) | H-$2^{d}$ | Haemolytic anemia; Glomerulonephritis; Lymphomas | 18 months | Both males and females equally | Production of anti-erythrocyte antibodies; Hyperproduction of IgM; Generalized Lymphocyte Dysfunction |
| BWF1 [F1 of (NZB x NZW)] | H-$2^{d/Z}$ | Severe Immune Complex-Mediated Nephritis | 7-8 months | Females | Production of Anti-Nuclear and Anti-DNA Antibodies; Generalized Lymphocyte Dysfunction |
| MRL-*LPR/LPR* | H-$2^{k}$ | Lymphoproliferation; Immune Complex-Mediated Nephritis;Rheumatoid Arthritis; Vasculitis | 2-4 months | Females | Production of Anti-Nuclear Antibodies and Rheumatoid Factors; Proliferation of $Ly1^{+}$ cells; Generalized Lymphocyte Dysfunction |
| MRL+/+ | H-$2^{k}$ | Lymphoproliferation; Immune Complex-Mediated Nephritis;Rheumatoid Arthritis; Vasculitis | 18 months | Females | Production of Anti-Nuclear Antibodies and Rheumatoid Factors; Proliferation of $Ly1^{+}$ cells[a]; Generalized Lymphocyte Dysfunction |
| BXSB | H-$2^{b}$ | Haemolytic anaemia; lymphadenopathy, glomerulonephritis. | 2-4 months | Males | Production of anti-DNA antibodies, anti-NTA and ; anti-erythrocyte antibodies; thymic atrophy occurs earlier; than normal |
| Moth-eaten | H-$2^{b}$ | Hair loss, glomerulonephritis, increased susceptibility to infections. | 1 month | Both sexes are affected equally | Production of anti-DNA antibodies, anti-NTA and ; anti-erythrocyte antibodies; immunesuppresion |
| Palmerston–North | H-$2^{q}$ | Polyarteritis nodosa, immune-complex-mediated nephritis | 11 Months | Females | Production of anti-DNA antibodies; hyperreactivity of B lymphocytes |
| Swan | H-$2^{k}$ | Mild glomerulonephritis | 18 months | both sexes affected equally | Production of anti-DNA antibodies, thymic atrophy occurs earlier than normal. |
| SNF1 | H-$2^{q/d}$ | Severe glomerulonephritis | 4–8 months | Females | Production of anti-DNA antibodies and anti-nucleosome antibodies. |

## Clinical Scoring

The NIH developed an activity and chronicity index for renal biopsies.

Histologic features of activity, in glomeruli, are:
(1) cellular proliferation,
(2) fibrinoid necrosis,
(3) cellular crescents,
(4) hyaline thrombi or wire loops, and
(5) leukocyte infiltration, and, within the tubulointerstitium,
(6) mononuclear cell infiltration.

Features of chronicity, in the glomeruli, are:
(1) sclerosis and
(2) fibrous crescents and, within the tubulointerstitium,
(3) interstitial fibrosis and
(4) tubular atrophy.

Each histologic feature is graded on a scale of 0, 1, 2, or 3 for absent, mild, moderate, or severe. Therefore, the maximum chronicity score is 12, and the maximum activity score is 24 (fibrinoid necrosis and cellular crescents are weighted by a factor of 2).

The NIH indices for nephritis have emphasized multiorgan clinical disease activity indices, such as:

1. The Systemic Lupus Activity Measure (SLAM),
2. Lupus Activity Index (LAI), or
3. SLE Disease Activity Index (SLEDAI): The SLEDAI is designed to measure the activity or extent of inflammation in nine organ systems. It has a theoretical maximum of 105 points.
4. Creatinine in urine

# IN VITRO AND IN VIVO DIABETES MODELS

## Scope of Services

We offer standard and unique animal model studies for diabetes to include:

- Rodent Diabetes models
- Swine induced diabetes models (short term and long term)
- Islet transplantation rodent and swine models
- Device implantation and monitoring

P.O. Box 910418, San Diego, CA 92191
Phone: (858) 605-5882 • Toll Free: (866) 599-3019 • Fax: (858) 605-5916
www.btsresearch.com

## Type I and II Diabetes Animal Models

BTS Research offers mouse, rat and minipig streptozotocin or alloxan-induced insulin dependent Type I diabetes. The reproducibility and the induction of high levels of diabetes in animals are key requirement for successful use of such animal models for drug discovery and development purposes.

BTS Research uses over 1000 rodent and over 30 pigs and minipigs a month making us one of the largest if not the largest CRO in the business of Type I diabetes. The induced IDDM in minipigs closely mimics the type 1 diabetes of humans. Because of the similarities between swine and humans, the induced diabetes can be monitored and controlled using the same protocols as in humans.

In addition, BTS Research offers low dose repeated insulin independent streptozotocin-induced Type II diabetes in rodents and minipigs. Zucker rats, obese diabetic (ob/ob) mice and. non-obese diabetic (NOD) mice are also offered.

Below is an example of Streptozotocin-induced Type I Diabetes in the Yucatan minipig performed by our staff at BTS Research.

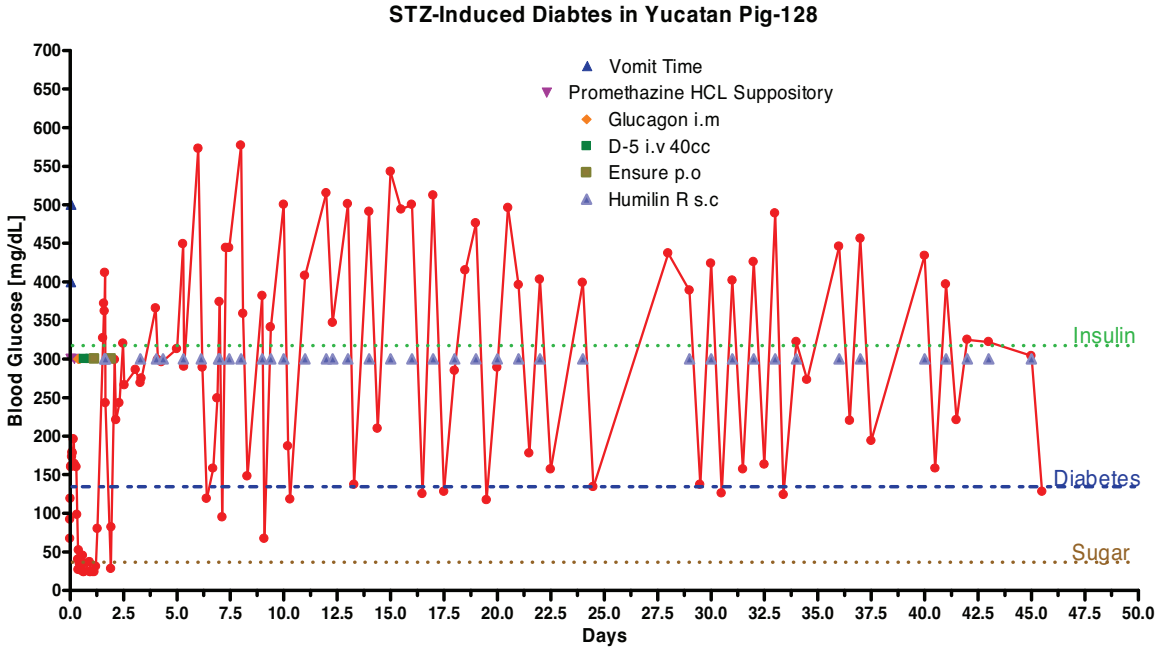


P.O. Box 910418, San Diego, CA 92191
Phone: (858) 605-5882 • Toll Free: (866) 599-3019 • Fax: (858) 605-5916
www.btsresearch.com

## BLOOD, URINE, CLINICAL CHEMISTRY, AND SPECIAL BIOCHEMISTRY PARAMETERS

We perform in house all routine and special clinical biochemistry tests for glucose, lipids (HDL / LDL, triglycerides, free fatty acids and cholesterol), insulin, GLP-1, leptin, amylin and ghrelin using both enzymatic and antibody based assays.

At experiment termination we also perform body-composition analyses (chemical or manual dissection of different fat-depots) and removal and preservation of blood / organs for subsequent analyses.

BTS Research is equipped with in house analyzers.

- Hematology
- Urinanalysis
- Clinical chemistry

## IMMUNOLOGY, CELL BIOLOGY, AND MOLECULAR BIOLOGY SUPPORT SERVICES

We also offer a wide range of immunological, cellular and molecular biology services. These services can be used in target validation studies; tissues can be harvested from in vivo studies and subsequently analyzed for drug-effects.

BTS Research offers extensive specific biomarker analysis for mouse, rat, swine, and monkeys to include:

- IL-1β, IL-2, IL-4, IL-5, IL-6, IL-10, IL-12
- TNF-α, IFN-γ, TGF-β
- MCP-1, MIP-1α, IL-8
- VEGF, IFG, FGF
- CRP

We have extensive experience with RNA and DNA isolation from all bodily tissues (including different fat compartments and pancreas) to determine mRNA expression levels.

Immunological and cellular in vitro assays include:

- Beta cell isolation
- Beta cell viability and characterization (western blot, FACS)
- Stress-induced and stimulus-induced insulin release
- Apoptosis and necrosis assays
- Effect of cytokines on beta cell function
- Effect of host cells on beta cell function

## LARGE ANIMAL SURGERY

BTS Research houses a well equipped large animal surgery room qualified for both terminal and non-terminal surgeries. Our staff is experienced in diabetes related surgeries such as pancreatectomies, islet transplantation (GVHD), and device implantation and monitoring.

## IN VIVO PHARMACOLOGY

With our skilled technical staff and scientific expertise, BTS Research offers high quality behavioral and physiological measurements.

Compounds can be administered by all routes (IP, PO, SC, ICV and IV) and in either acute or chronic (once or twice daily for months) settings.

Food, water and body-weight can be monitored on a daily / weekly basis or as needed basis. Locomotor activity can be accurately assessed and recorded for shorter or longer periods.

A number of different feeding paradigms are employed (metabolic manipulations – high or low energy, overfeeding, restricted feeding, or scheduled feeding). Physiological measurements include:

- Oral Glucose Tolerance Tests (OGTT, IVGTT and IGTT)
- Euglyceamic hyperinsulinaemic clamp
- Telemetric measurement of body-temperature, heart-rate, blood-pressure and indirect calorimetry.

# IN VIVO WOUND HEALING MODELS

## Scope of Services

- Rodent wound healing models
- Swine wound healing model (short term-9 day, long term-21 day, surface and full thickness/deep seeded)

P.O. Box 910418, San Diego, CA 92191
Phone: (858) 605-5882 • Toll Free: (866) 599-3019 • Fax: (858) 605-5916
www.btsresearch.com

## INTRODUCTION

The response to injury is a phylogenetically primitive, yet essential innate host immune response for restoration of tissue integrity. Tissue disruption in higher vertebrates, unlike lower vertebrates, results not in tissue regeneration, but in a rapid repair process leading to a fibrotic scar. Wound healing, whether initiated by trauma, microbes or foreign materials, proceeds via an overlapping pattern of events including coagulation, inflammation, epithelialization, formation of granulation tissue, matrix and tissue remodeling. The process of repair is mediated in large part by interacting molecular signals, primarily cytokines, that motivate and orchestrate the manifold cellular activities which underscore inflammation and healing (Figure 1).

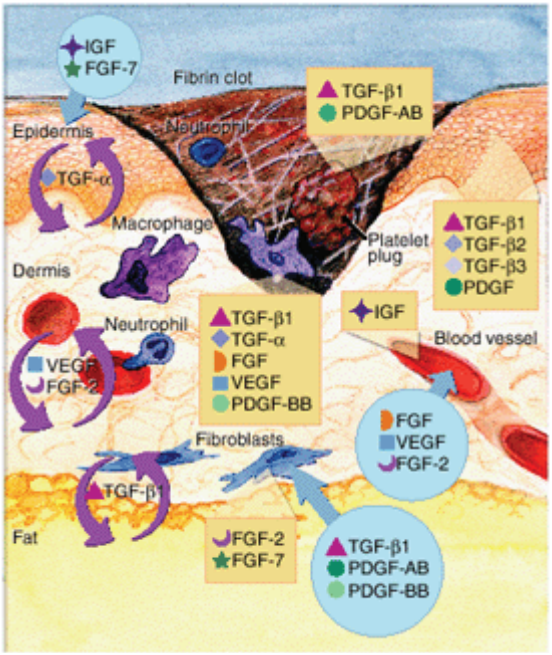


**Fig. 1.** Wound healing is a complex process encompassing a number of overlapping phases, including inflammation, epithelialization, angiogenesis and matrix deposition. During inflammation, the formation of a blood clot re-establishes hemostasis and provides a provisional matrix for cell migration. Cytokines play an important role in the evolution of granulation tissue through recruitment of inflammatory leukocytes and stimulation of fibroblasts and epithelial cells. [Note: figure is adapted from reference 1.]

Response to injury is frequently modeled in the skin,[1] but parallel coordinated and temporally regulated patterns of mediators and cellular events occur in most tissues subsequent to injury. The initial injury triggers coagulation and an acute local inflammatory response followed by mesenchymal cell recruitment, proliferation and matrix synthesis. Failure to resolve the inflammation can lead to chronic nonhealing wounds, whereas uncontrolled matrix accumulation, often involving aberrant cytokine pathways, leads to excess scarring and fibrotic sequelae. Continuing progress in deciphering the essential and complex role of cytokines in wound healing provides opportunities to explore pathways to inhibit/enhance appropriate cytokines to control or modulate pathologic healing.

The process of wound repair differs little from one kind of tissue to another and is generally independent of the form of injury. Although the different elements of the wound healing process occur in a continuous, integrated manner, it is convenient to divide the overall process into three overlapping phases and several natural components for descriptive purposes.

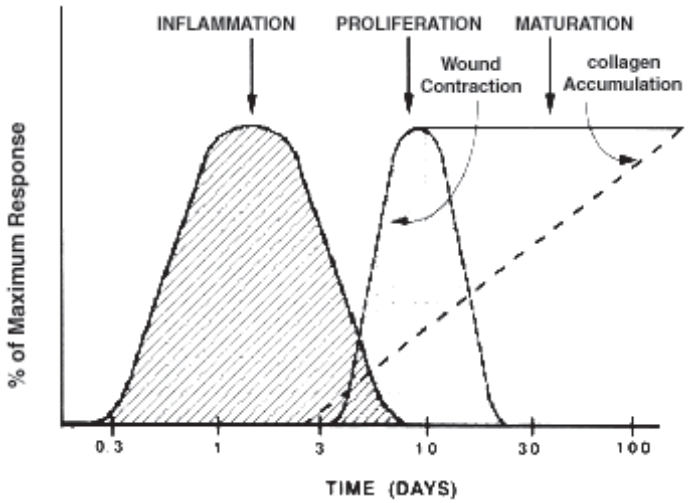


**Fig. 2.** Phases of wound repair. Wound healing has been arbitrarily divided into three main phases: inflammation, proliferation and maturation

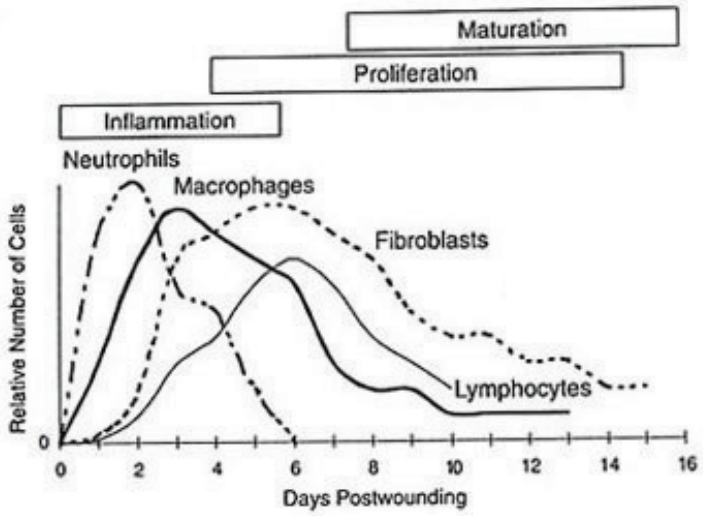


**Fig. 3.** Cells involved in Phases of wound repair. Wound healing has been arbitrarily divided into three main phases: inflammation, proliferation and maturation

P.O. Box 910418, San Diego, CA 92191
Phone: (858) 605-5882 • Toll Free: (866) 599-3019 • Fax: (858) 605-5916
www.btsresearch.com

## LARGE ANIMAL SURGERY

BTS Research houses a well equipped large animal surgery room qualified both terminal and non-terminal surgeries. Our staff is experienced in wound healing models, both surface and deep seeded in rodents and pigs.

## IN VIVO PHARMACOLOGY

With our skilled technical staff and expert scientific knowledge BTS Research offers high quality behavioral and physiological measurements. Compounds can be administered by all routes (IP, PO, SC, ICV and IV) and in either acute or chronic (once or twice daily for months) settings.

Food, water and body-weight can be monitored on a daily / weekly basis. Locomotor activity can be accurately determined for shorter or longer periods.

### Wound Healing Animal Models

BTS Research uses over 1000 rodent and over 60 pigs and minipigs a month making us of the largest if not the largest CRO in the business of wound healing.

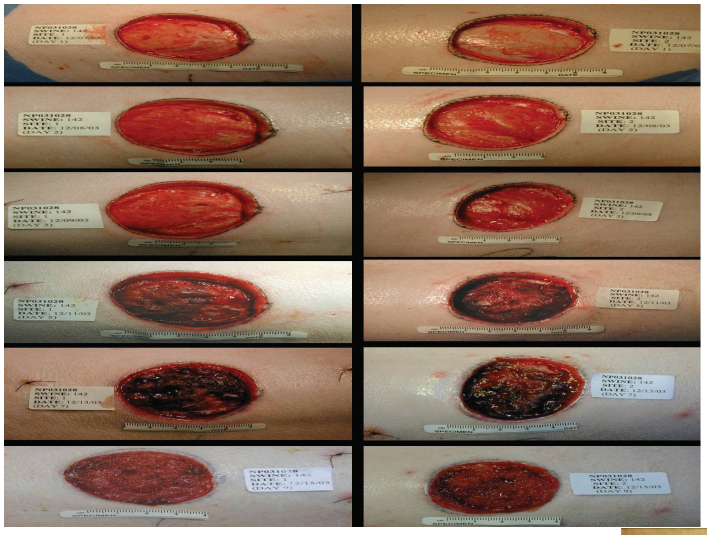

BTS Research offers rat and pig surface and full thickness/deep seeded wound healing models. The reproducibility of the wound healing is a key requirement for successful use of such animal models for drug discovery and development purposes. The full thickness wound healing model is offered in the pig or minipig with up to 21-day for closing and healing.

To the right hand are pictures from an in house experiment using the Yorkshire for the deep wound healing model. Closure of the wound takes place between 9-12 days and the wound fully heals at 21-25 days. Topical (gel, cream, liquid) and systemic drug formulation can be tested in this model.

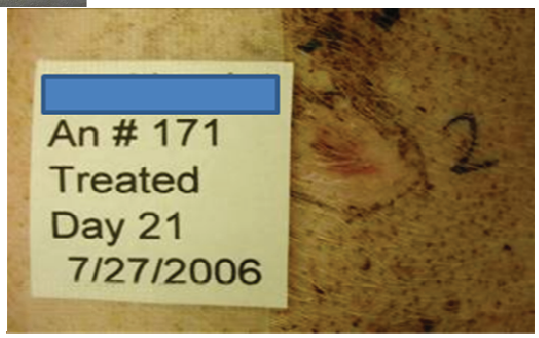


P.O. Box 910418, San Diego, CA 92191
Phone: (858) 605-5882 • Toll Free: (866) 599-3019 • Fax: (858) 605-5916

## BLOOD, URINE, CLINICAL CHEMISTRY, AND BLOOD BIOCHEMISTRY

BTS Research is equipped with in house analyzers for hematology, urine and clinical chemistry of samples.

## IMMUNOLOGY, CELL BIOLOGY, AND MOLECULAR BIOLOGY SERVICES

We also offer a wide range of immunological, cellular and molecular biology services. These services can be used in target validation studies; tissues can be harvested from in vivo studies and subsequently analyzed for drug-effects.

Ex Vivo Assays:

We offer an extensive array of ex vivo assays from cell proliferation, cytokine release, cell function such as chemotaxis, activation, antibody production, B cell switching in addition to the standard cell function assays.

BTS Research offers extensive analyses of mouse, rat, swine, monkey, and human specific biomarkers including IL-1, IL-2, IL-4, IL-5, IL-6, IL-8, IL-10, IL-12, TNF-a, MCP-1, MIP-1a, IFN-g, TGF-b, and CRP done from serum/plasma and wound tissues.

We have extensive experience with RNA and DNA isolation from all bodily tissues (including different fat compartments and pancreas) to determine mRNA expression levels.


# IN VIVO AND VITRO ACNE RELATED ASSAYS AND ANIMAL MODELS

# IN VIVO ANIMAL MODELS

## Rhino Acne Mouse Model

**Time to Completion…….10-14 Weeks**

Rhino mice have normal-appearing skin and hair at birth. At the end of the first hair cycle in $hr^{rh}/hr^{rh}$ mice, the dermal papilla fails to follow the contracting follicle and becomes isolated in the reticular dermis and hypodermis. These do not become reassociated to start the hair cycle over again. By three weeks of age, small lumen develop that enlarge with age forming deep dermal cysts. Sebaceous glands undergo hypertrophy at 30 days of age and atrophy after 1 year of age. A mixture of cells, consisting of macrophages and giant cells, surround cornified material from ruptured dermal cysts. Meibomian glands are modified sebaceous glands located in the eyelids, and the changes in the meibomian glands parallel those observed in sebaceous glands. Corneas of $hr^{rh}/hr^{rh}$ mice have a white exudate that contains increased numbers of pre-exfoliative conrneal epithelial cells. Rhino mouse skin is deficient in triacylglycerol, similar to normal mouse skin. Rhino mice also lack stores of triacylglycerol in adipose tissue. Meibomian gland and corneal irregularities in the rhino mouse mutation have been suggested as potential models for studying the pathogenesis of human acne, eyelid margin disease or corneal dystrophy. The rhino mouse mutation is a useful model for studying the hair cycle, and may also be useful for investigating mechanisms of epidermal hyperplasia.

| | |
|---|---|
| Diseased Mice: | RHINO-M |
| Control Mice: | RHINO-T |
| Grouping: | 10 mice /group |
| # Groups: | 2 |

**Determinations:**

1. Weekly Weights
2. Clinical Scoring

# IN VITRO ASSAYS

## Introduction

Skin surface lipids (SSL), a very complex mixture of sebum mixed to small amounts of epidermal lipids, mantle the human epidermis, thus representing the outermost protection of the body against exogenous oxidative insults.

Human sebum contains squalene, wax esters, triglycerides, cholesterol esters, and possibly free cholesterol. The fatty acids of the ester lipids include species with chain branching or with unusual double-bond positions. The alcohol moieties of the wax esters contain unusual chain types similar to those of the fatty acids. Genetic and hormonal factors cause individual differences in sebaceous lipid composition. Genetic factors seem to influence the proportions of the various types of branched-chain fatty acids. Androgenic stimulation of the glands causes an increase in lipid synthesis, and therefore affecting the ratio of endogenously synthesized lipid to exogenous lipid. Because the endogenously synthesized lipids tend to be different from lipids that are derived exogenously, the overall composition of the secretion changes. Differences in sebum composition are particularly evident when the sebum of prepubertal children is compared with that of young adults. One difference that may be of clinical significance is the different concentrations of linoleate. Higher concentrations of sebum linoleate may protect young children from comedonal acne by preventing an essential fatty acid deficiency from developing in the follicular epithelium.

P. acnes, a bacterium that is normally found on the skin, hydrolyzes certain triglycerides to fatty acids, thereby changing the sebum composition

## Primary and Immortalized Sebocytes

### Cell lines:

SZ95, a line of human facial skin sebocytes, and SEB-1, a line of human sebaceous gland, have been immortalized by transfection of simian virus 40 large T antigen.

Generation of the SZ95 cell line: Human facial sebaceous gland cells were transfected with a PBR-322-based plasmid containing the coding region for the Simian virus-40 large T antigen. The resulting proliferating cell cultures have been passaged over 50 times to date, have been cloned, and show no signs of senescence after passages, whereas normal human sebocytes can only be grown for three to six passages. The immortalized transfected cells, termed SZ95, expressed the Simian virus-40 large T antigen and presented an hyper-diploid-aneuploid karyotype with a modal chromosome number of 64.5. The SZ95 cell line exhibited epithelial, polymorphous characteristics with different cell sizes of up to 3.25-fold during proliferation and 6-fold at confluence, showing numerous cytoplasmic lipid droplets. The cells showed large cytoplasm profiles with

abundant organelles, including vacuoles and myelin figures which indicated lipid synthesis. Lack of or only few desmosomal areas were observed. SZ95 cells expressed molecules typically associated with human sebocytes, such as keratins 7, 13, and 19, and several proteins of the polymorphous epithelial mucin family. Functional studies revealed synthesis of the sebaceous lipids squalene and wax esters as well as of triglycerides and free fatty acids, even after 25-40 passages; active lipid secretion; population doubling times of 52.4 +/- 1.6 h; reduced growth but maintenance of lipid synthesis under serum-free conditions; and retrieval of cell proliferation after addition of 5alpha-dihydrotestosterone. Retinoids significantly inhibit proliferation of certain SZ95 cell clones in the expected magnitude 13-cis-retinoic acid > all-trans-retinoic acid > > acitretin. Thus SZ95 is an immortalized human sebaceous gland cell line that shows the morphologic, phenotypic and functional characteristics of normal human sebocytes

Additional confirmation of the the sebaceous phenotype of the cells lines is confirmed using immunohistochemistry, Oil Red O staining, and gene array expression analysis. Presence of P450scc, adrenodoxin reductase, cytochrome P450 17-hydroxylase (P450c17), and steroidogenic factor 1 is documented in human facial skin, human sebocytes, and SEB-1 sebocytes.

**Primary human sebocytes:**

Sebaceous glands are isolated from dispase-treated facial skin specimens and cultured using two different methods, explant culture and dispersed cell culture, in KGM. In both types of culture, the sebocytes proliferate rapidly without a biological feeder layer or specific matrices. Cells can be serially cultured for at least three passages (explant culture) and six passages (dispersed cell culture), and can be stored in liquid nitrogen with good recovery. Analytical thin-layer chromatography shows that the cells synthesized a large amount of sebum-specific lipids, squalene and wax esters in vitro. Both testosterone and 5 alpha-dihydrotestosterone significantly stimulate the proliferation of the sebocytes.

## In Vitro Measurement of Sebum Lipids

Squalene, an isoprenoid and a cholesteroal precursor, is one of the main active components produced by the sebaceous gland and sebocytes and is indicative of sebum production.
Squalene is produced by both primary and immortalized sebocytes and is measured by chromatography.

## Screening of compounds against keratinocyte proliferation, sebocyte proliferation and sebum production

BTS Research offers low and high throughput screening of compounds that inhibit primary keratinocytes, immortalized keratinocytes, primary sebocytes, immortalized sebocyte proliferation and sebum secretion.

Keratinocytes Assay: Briefly, cells are cultured in 96-well tissue culture plates at a density of 20,000 cells per well for 24 h. The wells are then washed with PBS, and BSA-medium was added. After 2 days, the cells are harvested, and fresh BSA-medium with or without active compounds are added to the cells. MTT, MTS, or Brdu is added and absorbance as a quantitative indication of cell number surviving is measured.

Sebocytes Assay: Briefly, cells are cultured in 96-well tissue culture plates at a density of 20,000 cells per well for 24 h. The wells are then washed with PBS, and BSA-medium was added. After 2 days, the cells are harvested, and fresh BSA-medium with or without active compounds are added to the cells. MTT, MTS, or Brdu is added and absorbance is measured as a quantitative indication of the number of cells surviving. The supernatants are collected 24 h later and analyzed for squalene levels.

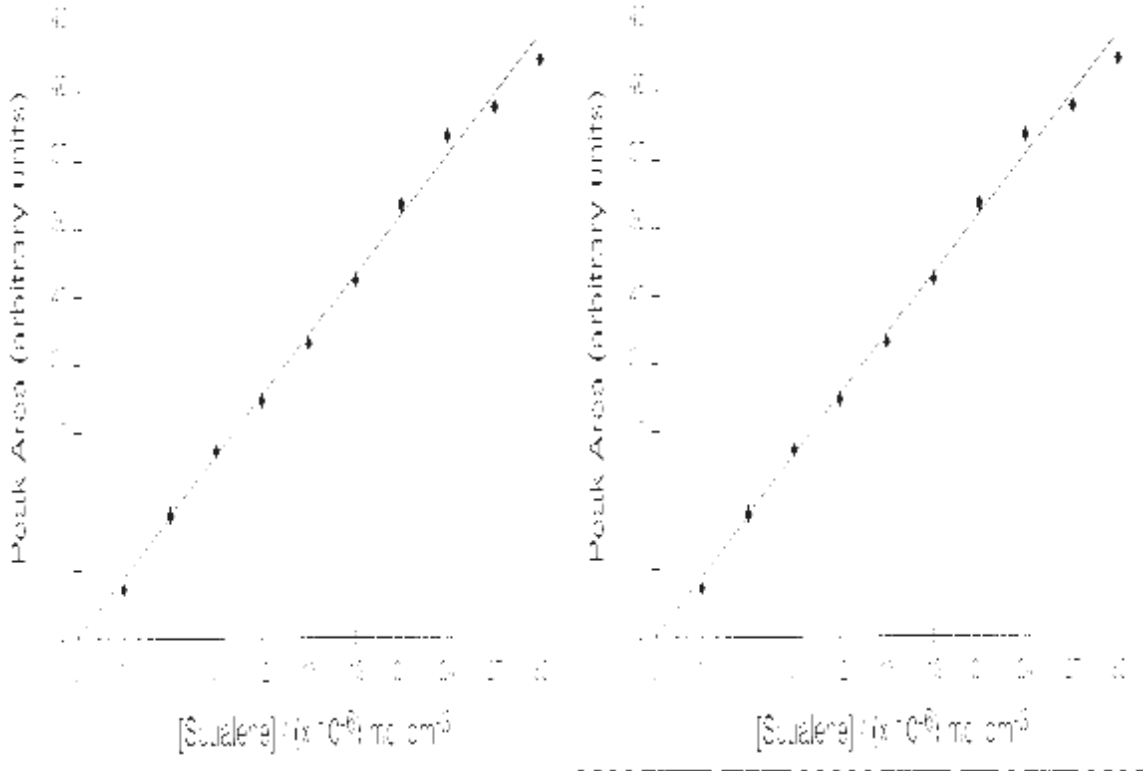


HPLC squalene calibration curve solubilized in water with propan-2-ol injected into acetonitrile (99.5%)/water (0.5%) HPLC mobile phase (1 ml min01 flow rate).

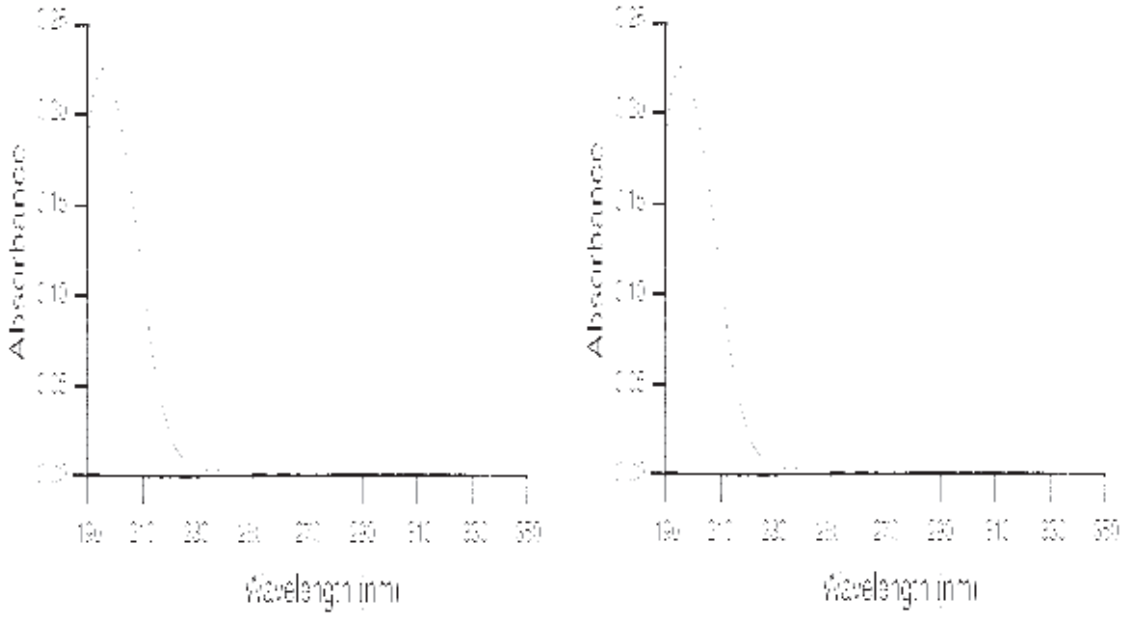


UV/visible spectrum for 4 mM squalene in acetonitrile (190– 350 nm)


# Spontaneous and Chemically Induced Liver Disease Models

# Lean and Ob Zucker Rats

**Time to Completion…….10-14 Weeks**

Nonalcoholic fatty liver disease (NAFLD) is the preferred term to describe the spectrum of liver damage ranging from hepatic steatosis to steatohepatitis, liver fibrosis, and cirrhosis, and it is emerging as the most common liver disease in industrialized countries. The ischemia-reperfusion (I/R) injury is an important cause of liver damage occurring during surgical procedures that include hepatic resections and liver transplantation. Hepatic steatosis is a major risk factor after liver surgery because steatotic livers tolerate poorly I/R injury. The occurrence of postoperative liver failure after hepatic resection in a steatotic liver exposed to normothermic ischemia has been reported. In addition, the use of steatotic livers for transplantation is associated with an increased risk for primary nonfunction or dysfunction after surgery.

Several hypotheses have been suggested to explain the decreased tolerance of steatotic liver to I/R injury compared with normal livers. These include increased 1) lipid peroxidation, 2) neutrophil infiltration, 3) microcirculatory alterations, and 4) release of proinflammatory mediators such as tumor necrosis factor (TNF)-α. Understanding the mechanisms of liver failure in steatotic livers will help to increase the tolerance of fatty livers to I/R injury and consequently decrease the inherent risk of liver surgery.

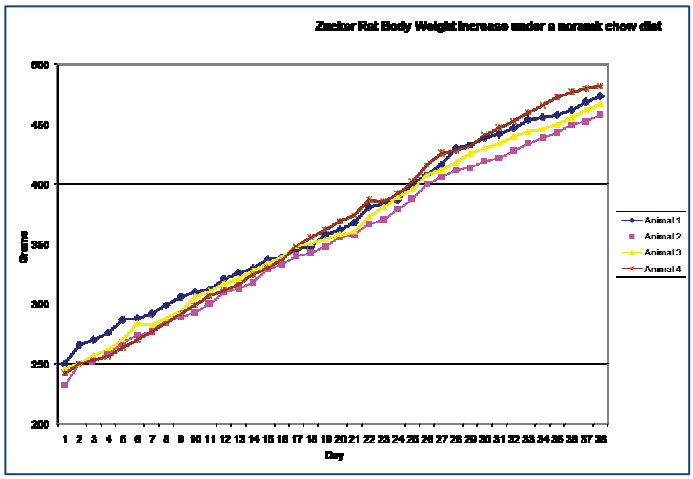


Several experimental models of NAFLD exist including the Zucker (*fa*/*fa*) rat. Zucker rats develop a syndrome with multiple metabolic and hormonal disorders that shares many features with human obesity. Zucker rats have hyperphagia, because they have a missense mutation on the leptin receptor gene; they become obese and develop hyperinsulinemia, diabetes, hypertension, and NAFLD. Therefore, Zucker rats are also a good model for Syndrome X, in which multiple risks cluster in an individual

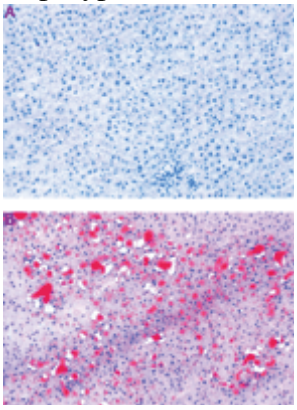

Zucker rats constitute a well-characterized model of nutritionally induced obesity and chemically (Methotrexate, 5-FU, Valproic Acid) induced liver injury. As previously reported, steatosis in Zucker rats is not associated with inflammation, as in other models of steatosis using ethanol ingestion or a choline-deficient diet. Homozygous Zucker rats (Obese, Ob) lack the cerebral leptin receptor and develop obesity at the age of 8

weeks because of markedly increased food intake and decreased energy expenditure. In contrast, heterozygous Zucker rats (Lean, Ln) have cerebral leptin receptors and maintain a lean phenotype throughout life. The difference of steatosis in the Ob (Figure A) *versus* Ln Zucker rats (Figure B) has been determined by using specific lipid staining such as red oil staining. Ob Zucker rats showed severe and macrovesicular and microvesicular fatty infiltration in hepatocytes (between 60% and 70% steatosis). In contrast, Ln Zucker rats show no evidence of steatosis

**Clinical End Points:**

1. Body Weight
2. Liver Weight
3. Measurement of lipid levels and hepatic injury marker activities in plasma: Triglyceride (TG), cholesterol, aspartate aminotransferase (AST), alanine aminotransferase (ALT), alkaline phosphatase (ALP), and lactate dehydrogenase (LDH)
4. Liver Histopathology with H&E and red oil staining for steatosis.

## Alcohol Induced Liver Damage in Lewis and Wistar Rats

Fatty infiltration, the first manifestation of alcohol-induced liver injury, is usually followed by inflammation, focal necrosis and terminal venular sclerosis, which ultimately can develop into cirrhosis. Steatosis was formerly considered a benign and fully reversible condition. However, new evidence suggests that hepatic fatty infiltration may in fact be an important pathogenic factor in the development of alcoholic liver disease (ALD). Both hepatic and extrahepatic factors, including peripheral lipolysis, enhanced hepatic fatty acid synthesis and reduced fatty acid oxidation, act together in the development of alcohol-induced fatty liver. For faster induction of liver damage, chemotherapeutic drugs such MTX and Valproic Acid are used to shorten the time to injury from 10 weeks to 3 weeks.

**Clinical End Points:**

1. Body Weight
2. Liver Weight
3. Measurement of lipid levels and hepatic injury marker activities in plasma: Triglyceride (TG), cholesterol, aspartate aminotransferase (AST), alanine aminotransferase (ALT), alkaline phosphatase (ALP), and lactate dehydrogenase (LDH)
4. Liver Histopathology with H&E and red oil staining.


# NON-GLP PHARMACOKINETIC (PK) AND PRECLINICAL TOXICOLOGY SERVICES

# Pharmacokinetic (PK)

Obtaining Pharmacokinetic (PK) data is a key requirement in the evaluation of new chemical entities. A quantitative measure of drug exposure is always needed for the sound interpretation of preclinical efficacy studies. PK data is also necessary before toxicology studies can be performed.
Our experienced staff has investigated a wide variety of small molecule drugs, peptides, and protein pharmaceuticals in both small and large animals.

## PK Studies

In a typical PK study, blood samples are obtained from test animals following a single, multiple doses or a timed perfusion. Plasma samples are separated and analyzed. Typically, if the drug is going to be administered orally, both an i.v. PK and an oral PK should be run. From these two studies both the bio-availability and the pharmacokinetics of the drug can be calculated. The data is also used to generate concentration vs. time curves and allow the determination of fundamental PK parameters such as Cmax, Tmax, T½, AUC, drug clearance, terminal elimination half-life, oral bioavailability and volume of distribution.

## Time Points

The time points (and hence the number of animals) depend on the compound, the route of administration, and its half-life. For a small molecule administered i.v., we would recommend 5 minutes, 15 minutes, then 1, 2, 4, 6, and 24 hr because the half-life is short and because it is given IV. On the other hand, for a monoclonal antibody that has a half-life of 10 days, there is no reason to do a number of time points on Day 1. In this case, we would look at 4 hr, 24 hr, and then days 2, 4, 7, 10, 14, 17, 21, and 28.

## High Throughput Cassette PK Screening

For high throughput PK screening of compounds, BTS Research offers cassette dosing of up to 5 compounds simultaneously a ssuming analytical methods allows differentiation. It should be noted that T1/2 is sometimes affected by the dose administered and by the number of points used for the non compartmental calculation. The expected correlation between single and cassette dosing is usually in the range of an r=0.602.

## PK Analysis in Diseased and Tumor Bearing Animals

Pharmacokinetics of small molecules can change in diseases animals and especially in tumor bearing animals. BTS Research offers PK analysis in diseases animals such as EAE (PLP induced in SJL, MOG induced in C57 mice, PLP induced in Lewis rats) and CIA (DBA mice and rats). In addition, we offer PK analysis in a number of nude mice bearing tumors (~400-500mm2).

## Delivery Methods

BTS Research's scientists are experienced with all standard delivery methods including:

- Oral (using capsules, tablets or oral gavage)
- Arterial
- Intravenous
- Continuous infusion using mechanical or osmotic pumps
- Intramuscular
- Intraperitoneal
- Subcutaneous
- Nasal Mucosa, Nasal Cavity or Tracheal
- Bronchial (Inhaled Aerosols)

## Animal Species Offered

BTS Research offers PK studies in the following animal species:

1. Mice
2. Rats
3. Guinea Pigs
4. Hamsters
5. Ferrets
6. Pigs (domestic and minipigs)
7. Dogs
8. Cats
9. Gerbils
10. Rabbits

## PK Studies in Mice

A mouse PK study is a normally a terminal study in which sample collections are made by cardiac puncture (unless the assay allows for micro sample size where the mice can be bled more than once). For a mouse PK, we typically use 3-5 mice/sex for each time point.

## PK Studies in Rats

Rats can be bled up to seven times in a day in a PK study. To obtain more time points the groups can be divided accordingly. For example, 3-5 rats/subgroup and perhaps 2 subgroups per dose, (subgroup A bled at 0.5, 2 and 6 hr post dose and subgroup B bled at 1, 4, and 12 hr post dose). If the time points are very close together, we can pre-cannulate the rats to facilitate these bleeds. Because of the multiple bleeds, the number of rats will be about a seventh of that required for mice.

## PK Studies in Large Animals

BTS Research maintains colonies of large animals (dogs and pigs) for PK studies for use in dermal, oral, Sub-Q, and IV dosing. Many companies house large animals at our facility especially for their PK studies. This is a special service we offer, and in this case these animals are reserved for a customer's exclusive use. With larger animals, multiple bleeds can be made in a single day. Note that only 15% of the blood volume of the animal can be bled per day in a survival study. BTS Research has extensive experience in large animals, we typically use between 600-700 large animals in our studies per year.

# Preclinical Toxicology Studies

BTS Research's state-of-the-art facility specializes in contract performance of toxicology studies. Non-GLP toxicology studies are intended to provide preliminary assessment of a drug's safety. Non-GLP toxicology studies can be performed on research grade materials to reduce costs and promote study design flexibility. These early stage studies can be performed prior to committing to the substantial costs in time and financial resources required to producing GMP grade material.

## Toxicology Study Types

- Acute Toxicity (LD-50)
- Maximum tolerated dose (MTD)
- Single dose range-finding and acute toxicity studies
- Repeated Dose
- Sensitization
- Irritation

## Routes of Administration

All standard routes of administration are offered. Our strength is accommodating specialized client needs for treatment regimens.

- Subcutaneous
- Intraperitoneal
- Intravenous
- Intramuscular
- Topical
- Oral
- Controlled release pumps

## Species

BTS Research offers all standard test species. The following species can be housed at BTS Research's vivarium.

- Mouse
- Rat
- Hamster
- Guinea Pig
- Rabbit
- Dog
- Cat
- Gerbils
- Pig (Mini, Micro, Domestic)

# IN VITRO AND IN VIVO CANCER MODELS

## IN VITRO CANCER BIOLOGY SERVICES

BTS Research offers its clients several in vitro assays to help determine the efficacy, mechanism of action, and toxicity of their compounds. We have over 150 human and animal cell lines in house derived from such cancers as lung, stomach, colon, breast, prostate, ovary, liver, skin, leukemia, meningioma, schwanoma, and lymphoma. Whenever possible, we obtain cell lines from our clients to decrease non reproducible results due to variants arising from multiple passages of cells. If the client desires a specific cell line not in our library, we will determine its availability from sources such as the American Type Culture Collection (ATCC), DCTDC Tumor Repository (DCTDC), DSMZ Human and Animal Cell Cultures (DSMZ), ECACC European Collection of Cell Cultures (ECACC), Interlab Cell Line Collection (ICLC).

We offer in the following in vitro assays:

- Cell proliferation and growth inhibition assays (tumor and endothelial cells)
- Apoptosis assays (tumor and endothelial cells)
- Cell cycle and apoptosis analysis using flow cytometry
- Migration and invasion assays (Matrigel® and fibrin gel)
- Receptor binding and activity assays (ER, PR, AR, PPAR, etc.)
- ELISA, Western blots on treated animal tissue and cell lysates for enzymes, cytokines and other protein targets
- Zymogels for protease activity (MMPs, etc.)
- Biochemical assays for target effectiveness on treated animal tissues
- Custom in vitro assays

### In Vitro Cell Invasion Assay

The in vitro cell invasion assay is a colorimetric assay that utilizes an invasion chamber, which consists of a 24-well tissue culture plate and 12 cell culture inserts. The inserts contain an 8 µm pore size polycarbonate membrane, over which a thin layer of a solid gel of basement proteins prepared from the Engelbreth Holm-Swarm (EHS) mouse tumor, serving as an *in vitro* basement membrane is evenly layered. The ECM layer occludes the membrane pores, blocking noninvasive cells from migrating through. By contrast, invasive cells migrate through the ECM layer. The specific invasion of cells in response to compounds is the difference of the effects of the same compound on non invading cells minus its effects on invading cells

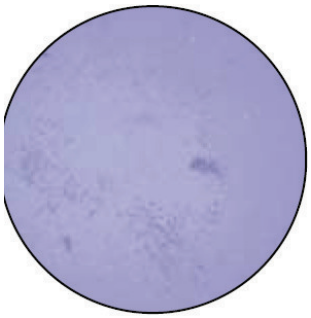

NIH3T3 non invading cells

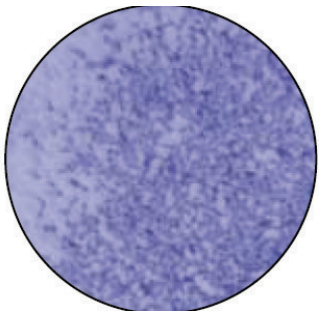

HT 1080 invading cells

**In Vitro Angiogenesis Assay**

The In Vitro Angiogenesis Assay allows for evaluation of tube formation by endothelial cells in a convenient 96- well microplate format. The assay utilizes, a solid gel of basement proteins prepared from the Engelbreth Holm-Swarm (EHS) mouse tumor. When placed in a 96-well tissue culture plate, this gel forms an *in vitro* analog of the basement membrane. Endothelial cells in solution are placed on top of the gel, allowing the cells to align and form tube-like structures which can be observed under an inverted light microscope. Tube formation is a multi-step process involving cell adhesion, migration, differentiation and growth.

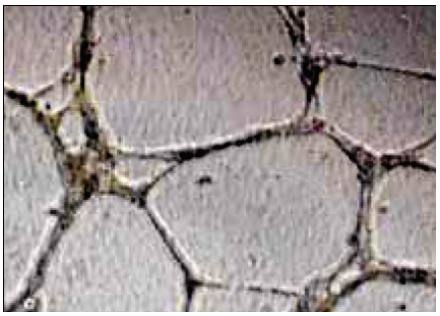

Tube formation (angiogenesis) by human endothelial cells in response to VEGF

**Soft Agar Colony Formation Assay**

The soft agar colony formation assay measures anchorage-independent growth of OVCAR-3 cells. Briefly, $10^5$ cells are suspended in 4 ml of DMEM supplemented with 10% calf serum and 0.4% Seaplaque agarose in 6-cm tissue culture plates containing 4 ml of 0.8% agarose containing DMEM underlay. Cultures will be fed with 0.2 ml of DMEM containing 10% of

calf serum twice a week for 2 weeks. The colonies will be stained with *p*-iodonitrotetrazolium violet after 2 weeks and photographed on an inverted light and counted.

**In Vitro Chemotaxis Assay**

The in vitro chemotaxis assay measures the migration of fluorescence labeled cancer cells across a polycarbonate filter in a 96 well chamber in presence or absence of chematactic agents. Compounds to be tested are added to upper and lower chambers to ensure a uniform presence of the inhibitors.

## Partial list of available cell cancer cell lines

| **Breast** | |
|---|---|
| BT-20 | Breast |
| BT-483 | Breast |
| BT-549* | Breast |
| HS 578T* | Breast |
| MB 157 | Breast |
| MCF7 | Breast |
| MDA-MB-134-VI | Breast |
| MDA-MB-157 | Breast |
| MDA-MB-175 | Breast |
| MDA-MB-175-VII | Breast |
| MDA-MB-231 | Breast |
| MDA-MB-361 | Breast |
| mda-mb-361 | Breast |
| MDA-MB-435 | Breast |
| MDA-MB-435s | Breast |
| MDA-MB-453 | Breast |
| MDA-MB-468 | Breast |
| MDA-n (not ava) | Breast |
| NCI/ADR-RES | Breast |
| T47D | Breast |
| T-47D | Breast |
| MDA-MB-134 | Breast |
| MDA-MB-153 | Breast |
| MDA-MB-436 | Breast |
| SK BR3 | Breast |

| **Cervix** | |
|---|---|
| Hela | Cervix |
| HeLa S3 | Cervix |
| Ca ski | Cervix |
| SiHa | Cervix |

| **CNS** | |
|---|---|
| CATH-A | CNS |
| SF-268 | CNS |
| SF-295 | CNS |
| SF-539 | CNS |
| SNB-19 | CNS |
| SNB-75 | CNS |
| D54MG | glioma |
| U251 | glioma |
| CNS | |
| NT2 | Neuron |

| **COLON** | |
|---|---|
| CaCO2 | Colon |
| Colo 201 | Colon |
| COLO 205 | Colon |
| DLD-1 | Colon |
| HCC-2998 | Colon |
| HCT-116 | Colon |
| HCT-15 | Colon |
| HT29 | Colon |
| HuT 78 | Colon |
| KM12 | Colon |
| LOVO | Colon |
| LS1034 | Colon |
| SP295 | Colon |
| SW 403 | Colon |
| SW 620 | Colon |
| SW 620 (P3) | Colon |
| SW1116 | Colon |
| SW480 | Colon |
| SW-620 | Colon |
| HCT 115 | Colon |

| **LIVER** | |
|---|---|
| C3A | liver |
| HepG2 | liver |

| **Leukemias** | |
|---|---|
| HL-60(TB) | Leukemia |
| RPMI-8226 | Leukemia B cell |
| Daudi | Leukemia B cell |
| Nanalwa | Leukemia B cell |
| RS11846 | Leukemia B cell |
| WSUNHL | Leukemia B cell |
| DOHH2 | Leukemia B cell |
| Karpas 299 | Leukemia B cell |
| SK-W64 | Leukemia B cell |
| THP-1 | Leukemia |
| Monocyte | |
| U937 | Leukemia |
| Monocyte | |
| K562 | Leukemia |
| Monocyte | |
| CCRF-CEM | Leukemia T cell |
| JURKATE6.1 | Leukemia T cell |
| Jurkat | Leukemia T cell |
| Jurkat CD26 | Leukemia T cell |
| Jurkat CD26 P14 | Leukemia T cell |
| Jurkat P17 | Leukemia T cell |
| Jurkat Parent | Leukemia T cell |
| Molt 4 | Leukemia T cell |
| SUD-HL4 | lymphoma |
| A2058 | Melanoma |
| LOX IMVI | Melanoma |
| M14 | Melanoma |
| MALME-3M | Melanoma |
| SK-MEL-2 | Melanoma |
| SK-MEL-28 | Melanoma |
| SK-MEL-5 | Melanoma |
| UACC-257 | Melanoma |
| UACC-62 | Melanoma |

| **Miscellaneous** | |
|---|---|
| T24 | human bladder |
| tumor cell line | |
| HT1080SQ1 | human |
| fibrosarcoma cell line | |
| HT1080SQ2 | human |
| fibrosarcoma cell line | |
| HPAEC-primary | Human |
| Pulmonary Artery Endothelial Cells (HPAEC) are isolated | |
| from normal human pulmonary arteries | |
| HUVEC | human umbilical |
| vein endothelial cells | |
| CPAE | Endothelial |
| 293T | Epithelial |
| 293 | Epithelia |
| A-204 | muscle |
| A-673 | muscle |
| nhek | Normal human |
| epidermal keratinocytes | |
| NHF | normal human |
| fibroblasts | |
| U2-OS | osteosarcoma |
| sw837 | rectum |
| SW13 | adrenal gland |
| Tissue: cortex primary small cell carcinoma | |

**Ovarian**

| | |
|---|---|
| Caov-3 | Ovarian |
| caov4 | Ovarian |
| ES-2 | Ovarian |
| igrov1 | Ovarian |
| IGR-OV1 | Ovarian |
| OV-90 | Ovarian |
| OVACAR 8 | Ovarian |
| OVACAR3 | Ovarian |
| OVCAR-4 | Ovarian |
| OVCAR-5 | Ovarian |
| OVCAR-8 | Ovarian |
| scov3? | Ovarian |
| SK-OV-3 | Ovarian |
| SW626 | Ovarian |
| TOV 21G | Ovarian |
| TOV112 | ovarian |
| PA-1 | ovarian |

**Pancreas**

| | |
|---|---|
| BxPC3 | Pancreas |
| MIA PaCa2 | Pancreas |
| NIAPACA2 | Pancreas |
| PANC 08.13 | Pancreas |
| PANC-1 | Pancreas |
| DU 145 | Pancreas |
| PC3 | Pancreas |

**Renal**

| | |
|---|---|
| 293/P9 | Renal |
| 786-O | renal |
| A498 | Renal |
| AcHn | Renal |
| CAKI-1 | Renal |
| RXF 393 | Renal |
| SN12C | Renal |
| TK-10 | Renal |
| UO-31 | Renal |

**Lungs**

| | |
|---|---|
| H460 | large cell |
| cancer of the lung | |
| A549/ATCC | Non-Small |
| Cell Lung cancer | |
| EKVX | Non-Small |
| Cell Lung cancer | |
| HOP-62 | Non-Small |
| Cell Lung cancer | |
| HOP-92 | Non-Small |
| Cell Lung cancer | |
| NCI-H226 | Non-Small |
| Cell Lung cancer | |
| NCI-H460 | Non-Small |
| Cell Lung cancer | |
| NCI-H522 | Non-Small |
| Cell Lung cancer | |
| H1299 | Non-Small |
| Cell Lung cancer | |
| NCI H1299 | Non-Small |
| Cell Lung | |
| Calu-6 | Non-Small Cell |
| Lung cancer | |
| DMS 79 | small cell lung |
| cancer | |
| NCI H146 | small cell lung |
| cancer | |
| NCI H146 | small cell lung |
| cancer | |
| NCI H209 | small cell lung |
| cancer | |
| NCI-H1688 | small cell lung |
| cancer | |
| NCI H220 | small cell lung |
| cancer | |
| H1299 | small cell lung |
| cancer | |
| H209 | small cell lung |
| cancer | |

**Murine /insects cells**

| | |
|---|---|
| ET26? | |
| HMVEC-D | |
| pc12(lg) | |
| WEHI 3B | |
| TA3ST | mouse |
| MEF-wt | mouse |
| SVEC | murine |
| NIH 3T3 | murine |
| SF-21 | insect cells |

| | |
|---|---|
| caco205 | |
| Danc1 | |
| H5578 | |
| H5578T | |
| H5S78T | |
| HCC 2995 | |
| HCC29986 | |
| jcd26 | |
| T1B-161 | |
| hcc290 | |
| hem | |
| HT/AP | |
| MoA468 | |
| SK5 | |
| THP1-n2 | |
| U031 | |
| U84MG | |
| U89MG | |
| 8W620clrf | |
| FL512 Neo | |
| FL512 WT | |
| NCI-H572 | |
| RPMI-A226 | |
| RS1184 | |
| SF-260 | |
| MCF-7 null | |
| NCTC Clone 929 Adapose | mouse |

# IN VIVO CANCER MODELS

## IN VIVO CANCER DRUG EFFICACY

BTS Research has three sites worldwide with over 40,000 s.q. of vivarium and laboratory space. Our animal facilities are located at the San Diego-Sorrento Valley site. From designing and performing animal studies and follow-up biochemistry experiments, our experienced staff works together with our clients to ensure that we provide the in vivo services they need. Our modern state-of-the-art animal facility includes suites dedicated to housing athymic mice, large animals including SPF animals, separate surgical suites, X-ray capabilities, and clinical CBC and chemistry analysis laboratories for evaluating the effect of test agents on the response of tumors to a multitude of chemical, biological, and radiation therapy.

**BTS Research is certified by:**

- USDA
- State of California
- EPA
- DEA
- OLAW

**Scope of Services**

We offer standard and unique animal model studies, including:

- Tumor Implants
- Human xenografts in nude athymic mice
- Syngeneic transplants in rats and mice
- Orthotopic and ectopic implantation
- Leukemia models (NOD/SCID)
- Metastasis Models
- Spontaneous metastasis
- Orthotopic and footpad implantation
- Intravenous injection
- Angiogenesis Models
- Leukemia Models

## EXAMPLES OF SOME IN VIVO: XENOGRAFT, SYNGENEIC TUMOR IMPLANTS, AND LEUKEMIA MODELS

### SOLID TUMORS

Human xenograft implants in nude athymic mice or syngeneic transplants in appropriate rodent models are the industry standard for assessing the success of an anti-cancer agent, whether the compound works by directly affecting the growth of the tumor or by controlling processes such as angiogenesis. Tumor cell cultures or tumor fragments are implanted either ectopically or orthotopically and the tumors grown to a specified size. The animals are randomized, placed into groups, and the test groups are treated with a prescribed drug regimen over the test period. Typically, tumor sizes are measured twice a week and body weight's once a wee k. The animals are sacrificed at the end of the test period and tissues are removed for pathological evaluation.

There are a number of sources for obtaining cancer cell lines (e.g., the American Type Culture Collection). Whenever possible, we like the client to supply the cell line so that the in vivo studies are performed from the same cell line source as the initial in vitro studies. Some human tumor lines that we commonly use in xenograft studies include:

- Breast (MDA-MB231, MCF-7)
- Lung (A549, DMS 79, H1688, H146, H889)
- Colon (HT25)
- Prostate (DU-145, PC-3)
- Ovary (Ovcar-3, SKOV-3)
- Brain (U87)
- Pancreas Adenocarcinoma (Panc 02.13)
- Fibrosarcoma (HT-1080)
- Leukemia (Several)
- Renal Carcinoma (Hs 835.T, Caki-2)
- Melanoma (A2058)

Examples of syngeneic cell lines include

- Mouse leukemia (L1210, P388)
- Mouse melanoma (B16)
- Rat gliosarcoma (9L)
- Rat mammary adenocarcinoma (R230)

## LEUKEMIA MODELS

### 1. HUMAN XENOGRAFT MET-1 ATL CELLS MOUSE MODEL (LENGTH OF STUDY DEPEND ON PERIOD OF TREATMENT)

- Female NOD/SCID mice are used in this model. The mice are used at the age of 6–12 weeks. Leukemia will be established by i.p. injection of 15 x $10^6$ freshly isolated MET-1 cells. Mice were randomly assigned to each group when their sIL-2Rα levels reached a range of 1,000–10,000 pg/ml serum. These levels were observed at approximately 10–14 days after tumor inoculation, at which time treatments will be initiated.

- The MET-1 cells are activated T cells from ALT patients that express high levels of CD3, CD4, CD25, CD122, and CD52.

- For the evaluation of therapeutic efficacy, groups of 10 NOD/SCID mice each will be injected with 10 million MET-1 leukemic cells i.p. and randomly assigned to groups that had comparable levels of the surrogate tumor marker, the serum sIL-2Rα (Tac, CD25). The groups of mice will be given PBS, Campath-1H, compound or the combination of Campath-1H and compound at a dose of 100 µg (4mg/kg) of each mAb i.v. weekly for 4 weeks and mice survival is recorded.

### 2. HUMAN XENOGRAFT MOLT-4 ATL CELLS IN THE FCR KO -/- MOUSE MODEL (LENGTH OF STUDY DEPEND ON PERIOD OF TREATMENT)

- Female FcR -/- NOD/SCID mice are used in this study. The mice are used at the age of 6–12 weeks. Leukemia will be established by i.p. injection of 15 x $10^6$ freshly isolated MOLT-4 cells. Mice were randomly assigned to each group when their sIL-2Rα levels reached a range of 40-100 pg/ml serum (mean 60 pg/ml). These levels were observed at approximately 10–14 days after tumor inoculation, at which time treatments will be initiated.

- The MOLT-4 cells are activated T cells from ALT patients that express high levels of CD3, CD4, CD25, CD122, and CD52.

- For the evaluation of therapeutic efficacy, groups of 10 FcR -/- NOD/SCID mice each will be injected with 10 million MET-1 leukemic cells i.p. and randomly assigned to groups that had comparable levels of the surrogate tumor marker, the serum sIL-2Rα (Tac, CD25). The groups of mice will be given PBS, Campath-1H, compound or the combination of Campath-1H and compound at a dose of 100 µg (4mg/kg) of each mAb i.v. weekly for 4 weeks and mice survival is recorded.

## 3. SYNHENEIC MOUSE AND RAT MODELS (LENGTH OF STUDY DEPEND ON PERIOD OF TREATMENT

Mouse and rat strains available include Nude (nunu), SCID, APCMin, Balb/C and C57/B1 mice, and Nude, FISHER and BD1X rats.

Examples of syngeneic cell lines include

- Mouse leukemia (L1210, P388)
- Mouse melanoma (B16)
- Rat gliosarcoma (9L)
- Rat mammary adenocarcinoma (R230)
- Rat T9 and F98 glioma cells
- Rat colon carcinoma cells (CC531)
- Rat Morris hepatoma (MH) and H9618a hepatoma cells
- Rat WB-2054-M5 colorectal cells

# Validation of Rat Glioma and Rat Colon Cancer models with Ritonavir and 5-FU

## F98 glioma cells Syngeneic Fischer Rat Model

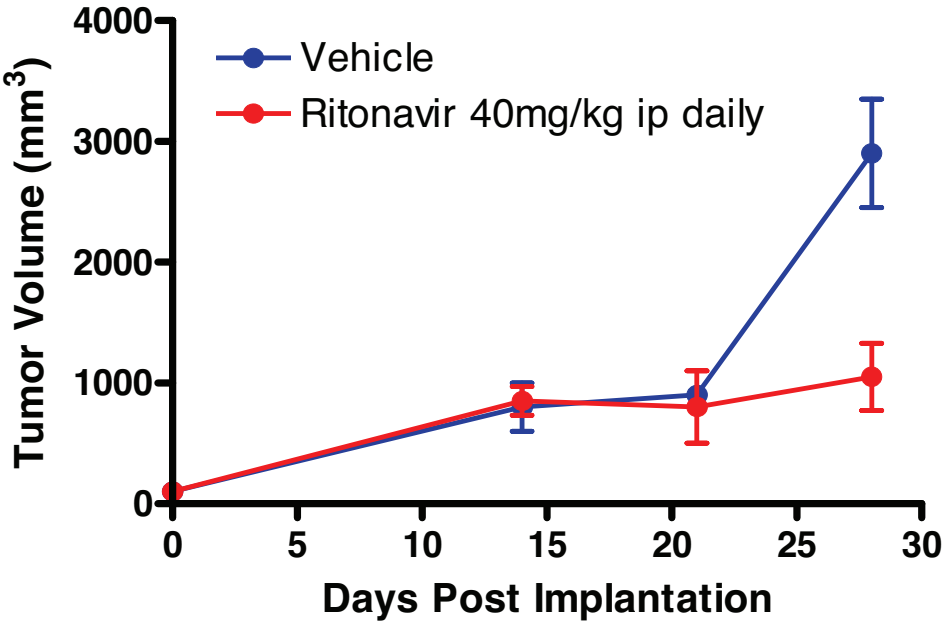


## WB-2054-M5 colorectal cells cells Syngeneic Fischer Rat Model

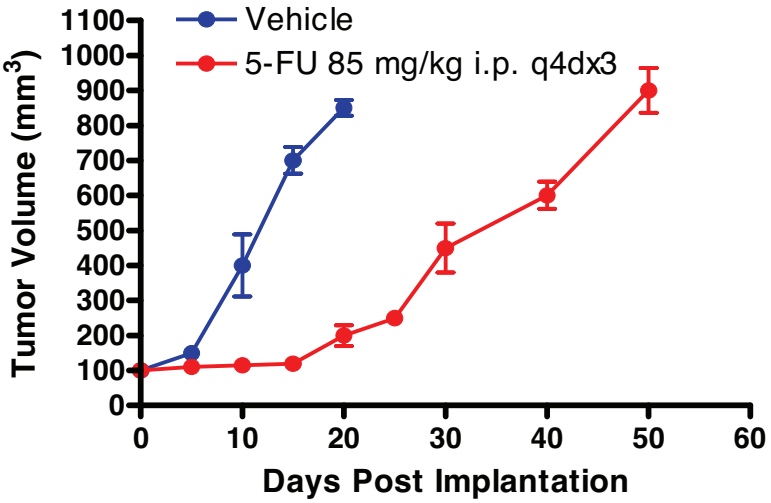

# Validation of MOLT-4 in the NOD/SCID mouse system with Campath

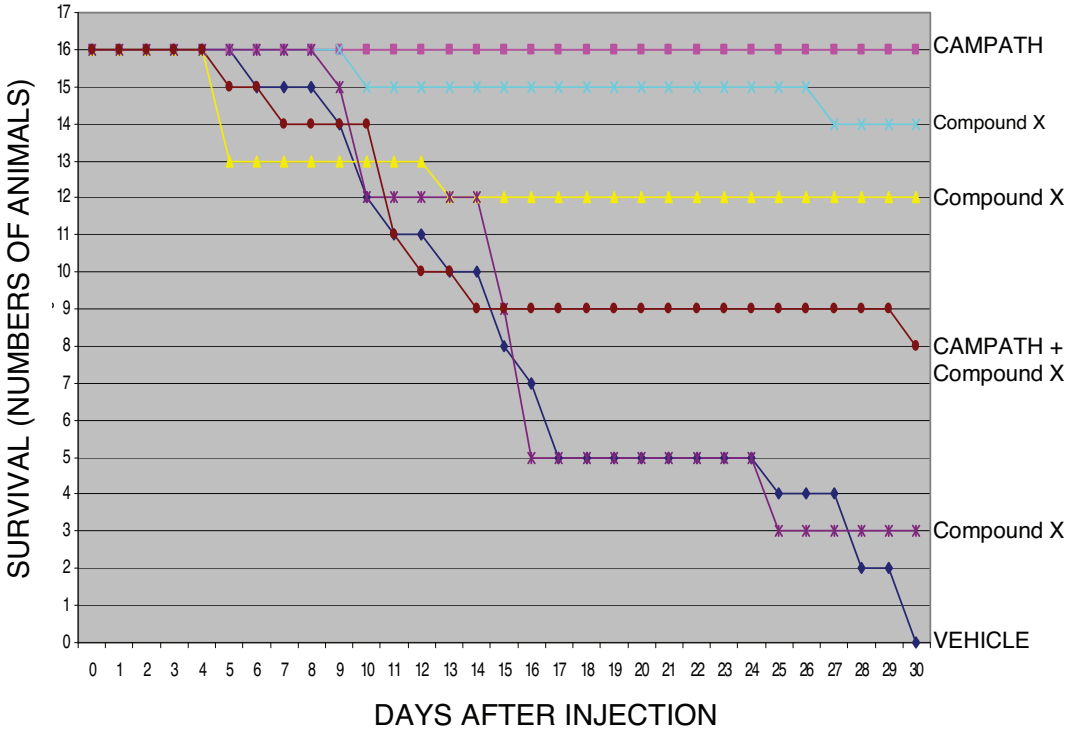


# BTS RESEARCH IN HOUSE CANCER CELL LINE COLLECTION

| Human Cell Lines | Description |
|---|---|
| 1301 | human blood leukemia acute lymphoblastic t-cell |
| 5637 | human urinary bladder carcinoma grade II |
| 786-O | human renal cell adenocarcinoma |
| A204 | human rhabdomyosarcoma |
| A2058 | human skin melanoma |
| A2780 | Human Ovarian Tumor |
| A3 | human melanoma |
| A-375 | human malignant melanoma |
| A431 | human skin epidermoid carcinoma |
| A498 | human renal cell carcinoma |
| A549 | human lung carcinoma |
| A549 | human lung |
| A673 | human muscle rhabdomyosarcoma |
| ACHN | human renal cell adenocarcinoma |
| ASG | human gastric adenocarcinoma |
| B2-17 | astrocytoma, thymidine kinase-deficient mutant of U251 MG cells, GFAP-negative |
| BE | |
| BT-20 | human breast carcinoma |
| BT-474 | human breast ductal carcinoma |
| BT-483 | human breast ductal carcinoma |
| BT549 | human breast ductal carcinoma |
| BxPC3 | human pancreas adenocarcinoma |
| BxPC-3 | human adenocarcinoma |
| C3A | human hepatocellular adenocarcinoma |
| CaCO2 | human colorectal adenocarcinoma |
| Caki1 | human kidney clear cell carcinoma |
| Calu-3 | lung adenocarcinoma |
| Calu-6 | human lung anaplastic carcinoma |
| CAMA-1 | human breast adenocarcinoma |
| CaOV3 | human ovary adenocarcinoma |
| CaOV4 | human ovary adenocarcinoma |
| Cath-a | human Brainstem tumor |
| CCRF-CEM | human acute lymphoblastic leukemia |
| CEMC1 | T lymphoblast, peripheral blood |
| CEMC2 | human leukemia T cell |
| Colo201 | human colorectal adenocarcinoma |
| Colo205 | human colorectal adenocarcinoma |
| COLO-206F | human colorectal adenocarcinoma |
| Colo677 | human colorectal adenocarcinoma |
| Colo775 | human colorectal adenocarcinoma |
| CPAE | human cultured pulmonary artery endothelial |
| CT26 | murine colon adenocarcinoma |
| CX-1 | human colon adenocarcinoma |
| D1.1 | human T cell leukemia |
| D54MG | human glioma |
| Daoy | human brain desmoplastic cerebellar medulloblastoma |
| Daudi | human B cell lymphoma |
| DC3 | rat granulosa cells |
| DG44 | human DHFR- CHO cells |
| DLD-1 | human colorectal adenocarcinoma |
| DMS 79 | human small cell lung cancer |
| DOHH2 | human EBV- B cell lymphoma |
| DU145 | human carcinoma; prostate; from brain |
| EKVX | human lung carcinoma |
| ES-2 | human clear cell carcinoma |
| Es5 | mouse embryonic stem cells |
| FL512 | human pro-B cell overexpressing Bcl-xs |
| G401 | human rhabdoid tumor (kidney) |
| GDM 1 | human acute myelomonocytic leukemia |
| H5578T | human breast tumor |
| H69AR | human lung epithelial carcinoma small cell lung cancer- multidrug resistant |
| H9 | human cutaneous T lymphocyte lymphoma |
| HCC290 | human colon adenocarcinoma |
| HCC2998 | human colon adenocarcinoma |
| HCT116 | human colorectal carcinoma |
| HCT-15 | human colorectal adenocarcinoma |
| HCT-8 | human colorectal adenocarcinoma |
| Hela | human colorectal adenocarcinoma |
| Hep 3B2.1-7 | human hepatocellular carcinoma |
| HEPG2 | human hepatocellular carcinoma |
| HL-60 | AML |
| HL-60 CLONE 15 | AML |
| HMVEC-D | human microvascular endothelial cell |
| HOP62 | human lung carcinoma |
| HOP92 | human lung carcinoma |

| Human Cell Lines | Description |
|---|---|
| HPAF-II | human pancreas adenocarcinoma |
| HRT-18 | human rectum-anus adenocarcinoma |
| Hs 602 | human cervical lymph node lymphoma |
| Hs 695T | human skin melanoma, amelanotic |
| Hs 700T | human pelvic adenocarcinoma |
| Hs 746T | human stomach gastric carcinoma |
| HS578T | human breast carcinoma |
| HT29 | human colorectal adenocarcinoma |
| HT-3 | human cervix carcinoma |
| HuT 78 | human T cell lymphoma |
| HuTu 80 | human duodenum adenocarcinoma |
| HUVEC | human umbilical vein endothelial cells |
| I 9.2 | human T cell leukemia |
| IGROV1 | human ovary adenocarcinoma |
| J GAMMA 1 | human T cell leukemia |
| J45.01 | human T cell leukemia |
| JEG-3 | human Placenta choriocarcinoma |
| JM1 | human T cell leukemia |
| Jurkat | human acute T cell leukemia |
| K562 | human chronic myelogenous leukemia |
| Karpas299 | human T cell lymphoma |
| KASUMI 1 | human myelobalst leukemia |
| KG 1 | human myelobalst leukemia |
| KM-12 | human colorectal adenocarcinoma |
| KM12LV5 | human colorectal adenocarcinoma |
| KNS-89 | gliosarcoma, GFAP and NSE-positive, S-100-negative |
| KPL-1 | human, japanese breast carcinoma |
| KU812 | Human leukemia |
| LN-18 | human cerebrum glioblastoma grade IV |
| LOXIMVI | human melanoma |
| LS 180 | human colorectal adenocarcinoma Dukes' type B |
| LUDLU-1 | human, caucasian lung carcinoma, squamous cell |
| M14 | Human melanoma |
| M14-NCI | |
| Malme-3M | human lung malignant melanoma |
| MAwi | human colorectal carcinoma |
| MC/CAR | human B lymphocyte plasmacytoma; myeloma |
| MC116 | human B lymphoma |
| MC3T3-E1 | human Bone preosteoblast |
| MCF7 | human breast adenocarcinoma |
| MCF-7 FAS | human MCF-7 transfected w/ FAS |
| MDAH2774 | human ovarian cancer |
| MDAMB157 | human breast carcinoma |
| MDAMB175 | human breast ductal carcinoma |
| MDAMB231 | human breast adenocarcinoma |
| MDAMB361 | human breast adenocarcinoma |
| MDAMB435 | human breast adenocarcinoma |
| MDAMB436 | human breast adenocarcinoma |
| MDAMB453 | human breast metastatic carcinoma |
| MDAMB467 | human breast adenocarcinoma |
| MDAMB468 | human breast adenocarcinoma |
| MEG01 | human chronic myelogenous leukemia |
| MiaPaca2 | human pancreas carcinoma |
| MO59K | human Brain malignant glioblastoma |
| MOLT3 | human T cell leukemia |
| MOLT4 | human T cell leukemia |
| MS751 | human cervix epidermoid carcinoma |
| MSTO-211H | lung biphasic mesothelioma |
| MV 4 11 | human B lymphoma |
| Namalwa | human lymphoblastoid |
| NCI/ADR-RES (MCF-7) | Human OvarianTumor |
| NCI-H128 | human carcinoma; small cell lung cancer |
| NCI-H1299 | human lung carcinoma |
| NCI-H1299 | human lung carcinoma |
| NCI-H1417 | human small cell lung carcinoma |
| NCI-H146 | human small cell lung carcinoma |
| NCI-H1463 | human non-small cell lung carcinoma |
| NCI-H1668 | human lung carcinoma |
| NCI-H1770 | neuroendocrine lung carcinoma |
| NCI-H196 | human variant small cell lung carcinoma |
| NCI-H1963 | human small cell lung carcinoma |
| NCI-H2126 | human adenocarcinoma; non-small cell lung cancer |
| NCI-H220 | human classic small cell lung cancer |
| NCI-H226 | human squamous cell carcinoma |
| NCI-H23 | non-small cell lung |
| NCI-H28 | human mesothelioma |
| NCI-H292 | human mucoepidermoid pulmonary carcinoma |
| NCI-H2998 | human colon |
| NCI-H322 | pulmonary bronchioloalvelar carcinoma |

| Human Cell Lines | Description |
|---|---|
| NCI-H378 | human lung carcinoma small cell lung cancer stage E |
| NCI-H460 | human lung carcinoma |
| NCI-H520 | human lung squamous cell carcinoma |
| NCI-H522 | human lung squamous cell carcinoma |
| NCI-H69 | human small cell lung carcinoma |
| NCI-H716 | human cecum colorectal adenocarcinoma |
| NCI-H82 | human small cell lung carcinoma |
| NCI-H820 | human papillary adenocarcinoma |
| NCI-N87 | human gastric carcinoma |
| NH17 | leukemia, acute lymphoblastic t-cell |
| NK92MI | human NK cells from non-hodgkins lymphoma |
| NR 8383 | human NK cells from non-hodgkins lymphoma |
| NT2 (NTERA-2) | human testicular carcinoma |
| NTERA | human testicular carcinoma |
| OV90 | human ovary adenocarcinoma |
| OVCAR 5 | human ovary adenocarcinoma |
| Ovcar-3 | human ovary adenocarcinoma |
| Ovcar-4 | human ovary adenocarcinoma |
| Ovcar-8 | human ovary adenocarcinoma |
| OVI-P | human ovarian cancer |
| P116 | human ovary adenocarcinoma |
| P39-TSU | acute myeloblastic leukemia |
| PA-1 | human ovary teratocarcinoma |
| PANC | human ovary teratocarcinoma |
| Panc-08.13 | human Pancreatic |
| Panc-1 | human pancreas carcinoma |
| Panc-10 | human Pancreatic |
| Panc-3 | human Pancreatic |
| PC3 | human prostate adenocarcinoma |
| Raji | Human B Lymphoma |
| Ramos | human B cell lymphoma |
| REH | human B cell lymphoma |
| RPMI 6666 | human B lymphoblastoma |
| RPMI 8226 | human B lymphoblastoma |
| RS1184 | human B lymphoma |
| RS11846 | human B lymphoma |
| RS4 11 | human leukemia |
| RXF-393 | Human renal |
| SAEC | Human Lung |
| SB12C | |
| SB295 | |
| SCC-25 | human tongue squamous cell carcinoma |
| SF21 | Human pupal ovarian cancer |
| SF263 | huma CNS |
| SF268 | huma CNS |
| SF295 | human CNS |
| SF539 | human CNS |
| SiHA | human cervix carcinoma |
| Ska-3-68 | human breast carcinoma |
| SKBr3 | human breast carcinoma |
| SK-BR-3 | human breast adenocarcinoma |
| SK-HEP-1 | human liver adenocarcinoma |
| SKMEL2 | human malignant melanoma |
| SKMEL28 | human malignant melanoma |
| SKMEL31 | human malignant melanoma |
| SKMEL5 | human melanoma |
| SK-N-BE(2) | human brain neuroblastoma |
| SK-N-DZ | human brain neuroblastoma |
| SK-OV3 | human ovary adenocarcinoma |
| SKS | human small cell carcinoma of the uterine cervix |
| SK-UT-1 | human uterus mesodermal tumor (mixed) grade III |
| SKW6.4 | human B lymphocyte |
| SN12C | human renal carcinoma |
| SN675 | human astrocytoma |
| SN75 | human astrocytoma |
| SNB19 | human CNS |
| SNB75 | human CNS |
| SNU-1 | human gastric carcinoma |
| SNU-C2B | human cecum colorectal carcinoma |
| SP295 | human glioblastoma multiform |
| SR | human human leukemia |
| SR-786 | anaplastic large t-cell lymphoma |
| ST486 | human lymphoma |
| SU.86.86 | human Pancreas ductal carcinoma |
| SUDHL4 | human follicular lymphoma |
| SVEC | Human endothelial |

| Human Cell Lines | Description |
|---|---|
| SW 1088 | human brain astrocytoma |
| SW 1990 | human pancreas adenocarcinoma |
| SW 780 | human urinary bladder transitional cell carcinoma |
| SW1116 | human colorectal adenocarcinoma Dukes' type A, grade III |
| SW13 | human adrenal gland carcinoma |
| SW1463 | human colorectal adenocarcinoma Dukes' type C |
| SW480 | human colorectal adenocarcinoma |
| SW527 | human colorectal adenocarcinoma |
| SW620 | human colorectal adenocarcinoma |
| SW626 | human ovary adenocarcinoma |
| SW756 | human cervix squamous cell carcinoma |
| SW837 | human rectum adenocarcinoma |
| SW948 | human colorectal adenocarcinoma Dukes' type C, grade III |
| T24 | human urinary bladder carcinoma |
| T47D | human breast ductal carcinoma |
| T84 | human colorectal carcinoma |
| T98G | human brain glioblastoma |
| TA3ST | human breast ductal carcinoma |
| TF1 | human brain glioblastoma |
| THP-1 | human acute monocytic leukemia |
| TK1 | Human renal |
| TK10 | Human renal |
| TOV-112D | human malignant ovary adenocarcinoma |
| TOV-21G | human malignant ovary adenocarcinoma |
| TR6BC1 | human malignant ovary adenocarcinoma |
| U-118 MG | human glioblastoma; astrocytoma-grade III |
| U251 | human malignant ovary adenocarcinoma |
| U251MG | human glioma |
| U266B1 | mouse schwannoma |
| U-373-MG | human brain glioblastoma |
| U87MG | human brain glioblastoma |
| U937 | human histiocytic lymphoma |
| UACC257 | human brain glioblastoma |
| UACC-62 | human melanoma |
| UO31 | human renal |
| V2-05 | |
| WERI-Rb-1 | human retinoblastoma |
| WiDr | colorectal adenocarcinoma |
| Y79 | human retinoblastoma |
| ZR-75-1 | human breast duct epithelial ductal carcinoma |

## MOUSE CELL LINES

| Cell Lines | Description |
|---|---|
| NIH-3T3 | mouse fibroblast |
| TA3ST | mouse carcinoma |
| B9 | mouse hybridoma |
| TR6Bc1 | mouse schwannoma |
| WEHI274.1 Y79 | mouse myelomonocytic leukemia |
| WEHI 3B "SK" | mouse myelomonocytic leukemia |

---

## RAT CELL LINES

| Cell Lines | Description |
|---|---|
| CC531 | rat colon carcinoma |
| H9618a | rat hepatoma |
| 9L | rat gliosarcoma, brain |
| F98 | rat undifferentiated malignant glioma |
| N1-S1 | rat hepatoma, liver |
| PC-12 | rat pheochromocytoma; adrenal gland |
| T9 | rat T-lymphoblastoid |
| WB-2054-M | rat carcinoma, colon |

---

## MONKEY CELL LINES

| Cell Lines | Description |
|---|---|
| COS-1 | monkey kidney fibroblast |
| COS-7 | monkey kidney fibroblast |

---

## RABBIT CELL LINES

| Cell Lines | Description |
|---|---|
| VX-2 | Rabbit renal carcinoma |
| VX-7 | Rabbit retinal carcinoma |


# In-House Validated Xenograft Mouse Models

**In House Validated Xenograft Mouse Models**

| Human Cell Lines | Description |
|---|---|
| 786-O | human renal cell adenocarcinoma |
| A431 | human skin epidermoid carcinoma |
| A498 | human renal cell carcinoma |
| A549 | human lung carcinoma |
| BT-474 | human breast ductal carcinoma |
| BxPC3 | human pancreas adenocarcinoma |
| C3A | human hepatocellular adenocarcinoma |
| CaCO2 | human colorectal adenocarcinoma |
| Caki1 | human kidney clear cell carcinoma |
| CaOV3 | human ovary adenocarcinoma |
| CaOV4 | human ovary adenocarcinoma |
| Cath-a | human Brainstem tumor |
| CCRF-CEM | human acute lymphoblastic leukemia |
| Colo201 | human colorectal adenocarcinoma |
| Colo205 | human colorectal adenocarcinoma |
| D54MG | human glioma |
| Daoy | human brain desmoplastic cerebellar medulloblastoma |
| Daudi | human B cell lymphoma |
| DC3 | rat granulosa cells |
| DG44 | human DHFR- CHO cells |
| DLD-1 | human colorectal adenocarcinoma |
| DMS 79 | human small cell lung cancer |
| DOHH2 | human EBV- B cell lymphoma |
| DU145 | human carcinoma; prostate; from brain |
| ES-2 | human clear cell carcinoma |
| G401 | human rhabdoid tumor (kidney) |
| H5578T | human breast tumor |
| H9 | human cutaneous T lymphocyte lymphoma |
| HCT116 | human colorectal carcinoma |
| HCT-15 | human colorectal adenocarcinoma |
| Hela | human cervix adenocarcinoma |
| HEPG2 | human hepatocellular carcinoma |
| HL-60 | |
| HT29 | human colorectal adenocarcinoma |
| HuT 78 | human T cell lymphoma |
| HUVEC | human umbilical vein endothelial cells |
| IGROV1 | human ovary adenocarcinoma |
| Jurkat | human acute T cell leukemia |
| K562 | human chronic myelogenous leukemia |
| Karpas299 | human T cell lymphoma |
| LN-18 | human cerebrum glioblastoma grade IV |
| LOXIMVI | human melanoma |
| LS 180 | human colorectal adenocarcinoma Dukes' type B |
| MC/CAR | human B lymphocyte plasmacytoma; myeloma |
| MCF7 | human breast adenocarcinoma |
| MCF-7 FAS | human MCF-7 transfected w/ FAS |
| MDAMB231 | human breast adenocarcinoma |
| MDAMB361 | human breast adenocarcinoma |
| MDAMB435 | human breast adenocarcinoma |
| MDAMB436 | human breast adenocarcinoma |
| MDAMB453 | human breast metastatic carcinoma |
| MDAMB467 | human breast adenocarcinoma |
| MDAMB468 | human breast adenocarcinoma |
| MiaPaca2 | human pancreas carcinoma |
| MOLT4 | human T cell leukemia |
| Namalwa | human lymphoblastoid |
| MV-411 | Leukemia |
| NCI/ADR-RES (MCF-7) | Human OvarianTumor |
| NCI-H1463 | human non-small cell lung carcinoma |
| NCI-H460 | human lung carcinoma |
| NCI-H520 | human lung squamous cell carcinoma |
| NCI-N87 | human gastric carcinoma |
| NT2 (NTERA-2) | human testicular carcinoma |
| NTERA | human testicular carcinoma |
| OV90 | human ovary adenocarcinoma |
| Ovcar-3 | human ovary adenocarcinoma |
| Ovcar-4 | human ovary adenocarcinoma |
| Ovcar-8 | human ovary adenocarcinoma |
| Panc-08.13 | human Pancreatic |
| Panc-1 | human pancreas carcinoma |

| Human Cell Lines | Description |
|---|---|
| Panc-10 | humanPancreatic |
| Panc-3 | humanPancreatic |
| PC3 | human prostate adenocarcinoma |
| Raji | Human B Lymphoma |
| Ramos | human B cell lymphoma |
| RPMI 8226 | human B lymphoblastoma |
| RS1184 | human B lymphoma |
| RS11846 | human B lymphoma |
| SCC-25 | human tongue squamous cell carcinoma |
| SKMEL2 | human malignant melanoma |
| SKMEL28 | human malignant melanoma |
| SKMEL31 | |
| SKMEL5 | human melanoma |
| SK-OV3 | human ovary adenocarcinoma |
| SNU-1 | human gastric carcinoma |
| SR | human human leukemia |
| SU.86.86 | human Pancreas ductal carcinoma |
| SUDHL4 | human follicular lymphoma |
| SW480 | |
| T47D | human breast ductal carcinoma |
| T98G | human brain glioblastoma |
| THP-1 | human acute monocytic leukemia |
| TK1 | |
| TK10 | Human renal |
| U-118 MG | human glioblastoma; astrocytoma-grade III |
| U251MG | human glioma |
| U87MG | human brain glioblastoma |
| U937 | human histiocytic lymphoma |
| ZR-75-1 | human breast duct epithelial ductal carcinoma |

# BIOMARKER QUANTITATIVE ANALYSIS

- BTS Research offers an extensive array of biomarkers quantitation by ELISA in multiple species.

- The main species we work with include:

    - Human
    - Monkey
    - Swine
    - Dog
    - Rat
    - Mouse

- Analysis is done in both serum and tissues.

| | | Species | | | | | |
|---|---|---|---|---|---|---|---|
| | Marker | Human | Monkey | Swine | Dog | Rat | Mouse |
| Cytokines | IL-1-β | √ | √ | √ | √ | √ | √ |
| | IL-2 | √ | √ | √ | | √ | √ |
| | IL-4 | √ | √ | √ | | √ | √ |
| | IL-5 | √ | √ | √ | | √ | √ |
| | IL-6 | √ | √ | √ | | √ | √ |
| | IL-10 | √ | √ | √ | | √ | √ |
| | IL-12 | √ | √ | √ | | √ | √ |
| | IL-13 | √ | √ | √ | | √ | √ |
| Chemokines | IL-8 | √ | √ | √ | | √ | √ |
| | Eotaxin | √ | √ | √ | | √ | √ |
| | MCP-1 | √ | √ | √ | | √ | |
| | JE | | | | | | √ |
| | CINC | | | | | √ | |
| | MIP-1α | √ | √ | √ | | √ | √ |
| | RANTES | √ | √ | √ | | √ | √ |
| Adhesion | VCAM-1 | √ | √ | √ | | √ | √ |
| | P-Selectin | √ | √ | √ | | √ | √ |
| | E-Selectin | √ | √ | √ | | √ | √ |
| Factors | VEGF | √ | √ | √ | | √ | √ |
| | M-CSF | √ | √ | √ | | √ | √ |
| | PF-4 | √ | √ | √ | | √ | √ |
| | TNF-α | √ | √ | √ | | √ | √ |
| | IFN-γ | √ | √ | √ | √ | √ | √ |
| | TGF-β | √ | √ | √ | | √ | √ |
| | FGF-2 basic | √ | √ | √ | | √ | √ |
| | PDGF | √ | √ | √ | | √ | √ |
| | IFG | √ | √ | √ | | √ | √ |
| | KGF | √ | √ | √ | | √ | √ |
| | MMP-9 | √ | √ | √ | | √ | √ |
| Inflammation | CRP | √ | √ | √ | | √ | √ |
| Immunoglobulins | IgG | √ | √ | √ | √ | √ | √ |
| | IgM | √ | √ | √ | √ | √ | √ |
| | IgA | √ | √ | √ | √ | √ | √ |


# IN VITRO & IN VIVO CARDIOCYTOTIXICITY SCREENS

# IN VITRO HUMAN CARDIOCYTOTIXICITY SCREEN™

## Introduction

Cardiac toxicity is a major concern in developing drugs for clinical use. Most of drug-induced cytotoxicity targets the heart muscles resulting in increased release of Lactate Dehydrogenase (LDH).

**BTS Research's In Vitro Human Cardio-Cytotoxicity Screen consists of 16 primary heart tissues for sign of cell death quantitatively by assessing the release of LDH at 24h and 48 hours in culture.**

**The human cardiac cell lines used for cardio-toxicity screening are:**

1. *Aortic Endothelial Cells (HAOEC):* HAOEC are primary endothelial cells isolated from normal human aorta
2. *Brachiocephalic Artery Endothelial Cells (HBcAEC):* HBcAEC are primary endothelial cells isolated from normal brachiocephalic arteries
3. *Brachiocephalic Artery Smooth Muscle Cells (HBcASMC):* HBcASMC are primary smooth muscle cells isolated from normal brachiocephalic arteries
4. *Carotid Artery Endothelial Cells (HCtAEC):* HCtAEC are primary endothelial cells isolated from normal carotid arteries
5. *Carotid Artery Smooth Muscle Cells (HCtASMC):* HBcASMC are primary smooth muscle cells isolated from normal brachiocephalic arteries
6. *Coronary Artery Endothelial Cells (HCAEC*): HCAEC are isolated from normal human coronary arteries
7. *Cardiac Fibroblasts (HCF):* HCF are derived from normal human heart tissue
8. *Pulmonary Artery Endothelial Cells (HPAEC):* HPAEC are isolated from normal human pulmonary arteries.
9. *Coronary Artery Smooth Muscle Cells (HCASMC*): HCASMC are derived from the tunica intima and tunica media of normal human, fibrous plaque-free coronary arteries
10. *Pulmonary Artery Smooth Muscle Cells (HPASMC):* HPASMC are derived from tunica intima and tunica media of normal human, fibrous plaque-free pulmonary arteries
11. *Aortic Smooth Muscle Cells (HAOSMC):* HAOSMC are derived from tunica intima and tunica media of normal human, fibrous plaque-free aorta.
12. *Internal Thoracic (Mammary) Artery Endothelial Cells (HITAEC):* HITAEC are derived from normal human internal thoracic arteries
13. *Internal Thoracic (Mammary) Artery Smooth Muscle Cells (HITASMC):* HITASMC are derived from the intrathoratic artery.
14. *Subclavian Artery Endothelial Cells (HScAEC):* HScAEC are derived from normal human subclavian arteries

15. *Subclavian Artery Smooth Muscle Cells (HScASMC):* HScASMC are derived from the subclavian artery
16. Myocardiocytes

**Price:**

- **Based on number samples and concentrations tested**
- **Performed in triplicates**

**Time to Completion:** 2-3 weeks

# IN VIVO CARDIOCYTOTIXICITY SCREEN™

**Introduction**

In the past few years, much attention has been focused on drugs that prolong the QT interval, potentially leading to malignant cardiac rhythm disturbances, such as torsade de pointes. Several drugs were withdrawn from the market (e.g., terfenadine, astemizole, cisapride, and grepafloxacin) because they either directly caused electrocardiographic abnormality or resulted in drug-drug interactions that led to unacceptable rates of cardiotoxicity. Hence, the need to assess the cardio-safety of drugs at an early stage is extremely important in furthering the development process.

Services Offered:

BTS Research is the only CRO on the West Coast that offers the non-invasive surface telemetry in freely roaming dogs to assess:

1. ECG, QT prolongation, Heart rate
2. Animal activity
3. Temperature

BTS Research surface telemetry allows the recording of the animal's signs continuously for up to 73 hours without interruption.

Additionally, we offer a cardiac blood panel to quantify the levels of:

1.LDH
2.SGOT
3.CPK
4.Myoglobin
5.Troponin I
6.C-reactive protein

**Price:**

- **Based on number of test articles**

**Time to Completion:** 2-3 weeks


# CaCO-2 Permeability Assay

A thorough understanding of intestinal epithelial transport is crucial for evaluating the potential for oral dosing of drug candidates. *In vitro* studies with CaCo-2 cell monolayers have proven to be a valuable tool for predicting human *in vivo* intestinal permeability.[1]

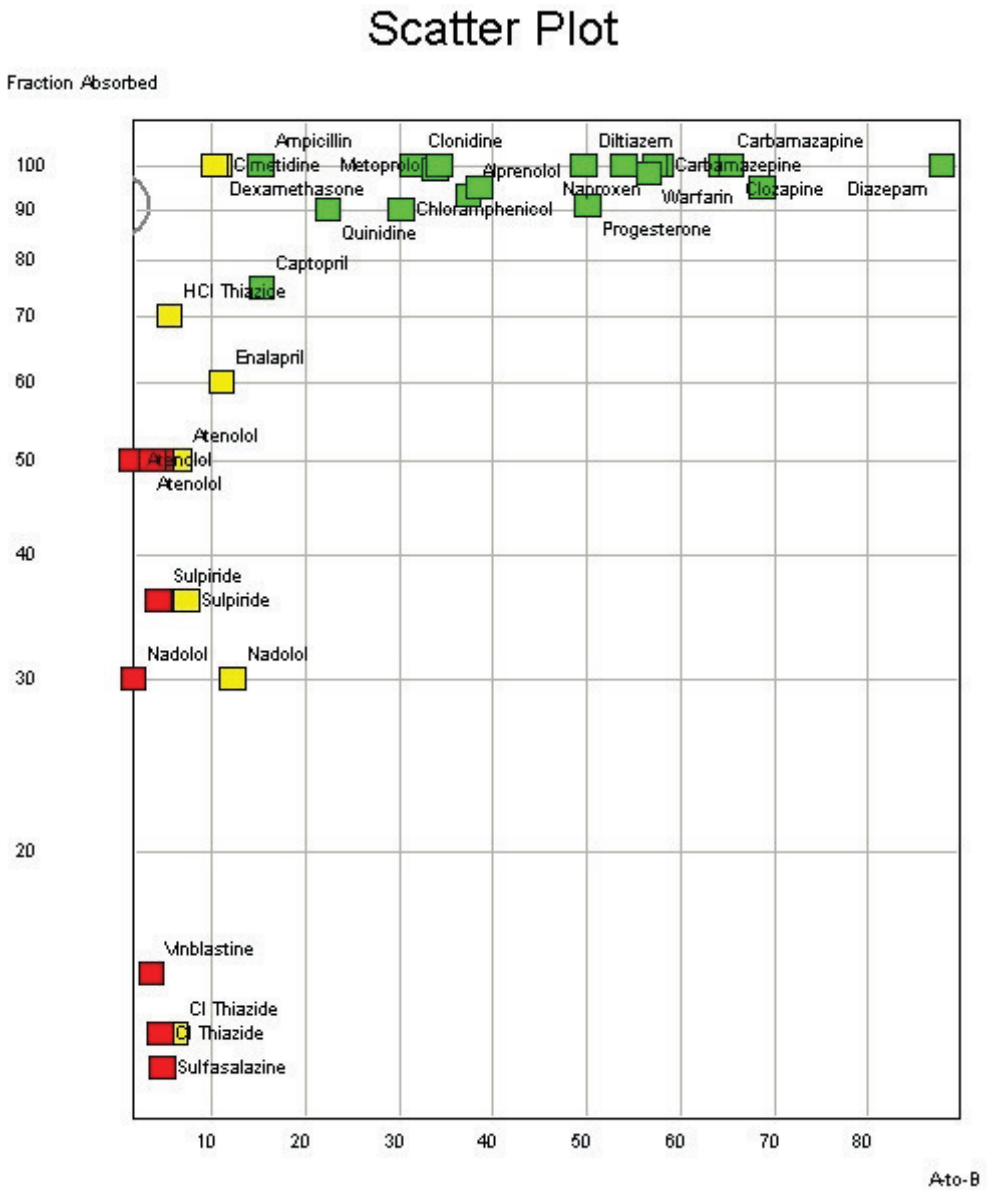


*Figure 1. Correlation of apparent permeability as measured at Apredica in the CaCO-2 permeability assay with reported human fraction absorbed (literature).*

*In vitro* permeability across differentiated monolayers of CaCO-2 cells is measured to estimate human intestinal permeability.

## CaCO-2 Cells as a Model of the Small Intestine for the Study of Drug Transport

Originally isolated from a colorectal carcinoma in the 1970s,[2] CaCO-2 cell monolayers spontaneously differentiate to express morphological and functional characteristics of mature small-intestinal enterocytes. The differentiated monolayers are polarized, with microvilli on the apical side, and express small intestinal hydrolase activities, including sucrase-isomaltase, lactase, aminopeptidases, on the apical surface.[3, 4] CaCO-2 cells grown on permeable filter supports form tight junctions and express transporters on the apical (e.g. P-gp[5, 6], MRP-2[6], BCRP[7]) and basolateral (e.g. MRP-1[6], PepT1[8, 9]) surfaces, and drugs that are predicted to be available are not transported across the intestinal mucosa due to the activity of efflux transporters.[10, 11] Permeability across CaCO-2 cell monolayers is used to predict human permeability of drug candidates, to perform in-depth mechanistic and absorption studies, to study the effects of transporters on permeability, and transporter-mediated drug-drug interactions. The CaCO-2 permeability assay is considered to be the industry gold standard for *in vitro* prediction of *in vivo* human intestinal permeability and bioavailability of orally administered drugs.[12] Fig. 1 represents a validation study conducted at Apredica on a subset of marketed drugs with fraction absorbed, reported in the literature. The FDA recommends that drug-drug interactions should be performed during drug development.[13]

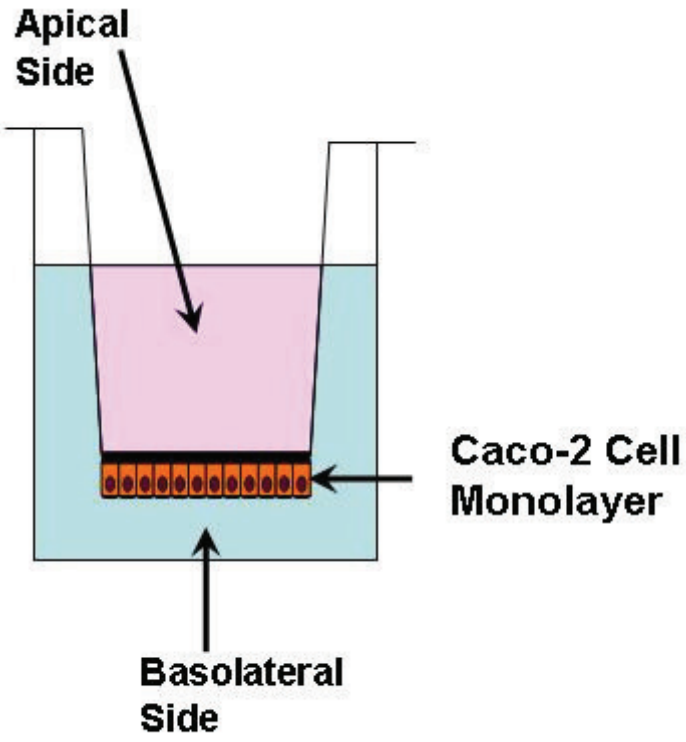


*Figure 2. Scheme of the CaCO-2 permeability assay.*

Permeability across differentiated monolayers of CaCO-2 is measured on fully differentiated cells grown for 3 weeks on permeable filter supports to estimate human intestinal permeability. The integrity of the monolayer is determined by measurement of TEER or by Lucifer Yellow permeability. Compounds are applied to the apical (A) or basolateral (B) side of the monolayer

and incubated for 2 h (Figure 2). The amount of compound on each side is measured by HPLC or LC/MS/MS. Permeability (Papp) is calculated in the apical to basolateral (A → B) and basolateral to apical (B → A) directions:

$$P_{app} = \frac{dQ/dt}{C_0 A}$$

where dQ/dt is the rate of permeation, C0 is the initial concentration of test agent, and A is the area of the monolayer.

Passively transported compounds show equal permeability in both directions. The role of transporters is demonstrated by asymmetry in the amount of permeability. A high B → A vs. A → B ratio indicates the possibility that the compound is an efflux transporter substrate. The transporter can be identified by performing the permeability assay in the presence of a specific inhibitor on both sides of the monolayer.

## Principle of the CaCO-2 Assay

CaCo-2 cells are grown to confluence and allowed to differentiate on filters. Test agent is added to one side of the monolayer, and permeability is assessed using HPLC or LC/MS.

## The CaCO-2 Cells

CaCO-2 human colon adenocarcinoma cells are grown to confluence and differentiated for 3 weeks on filters.

## CaCO-2 Assay Sample Requirements

20 µL of a 10 mM DMSO solution, based on a test concentration of 50 µM.

## CaCO-2 Assay Modes

**Screening**: Test agent is incubated for 2 hr on either side of the monolayer (apical and basolateral), and the concentration of the test agent on both sides is measured by HPLC or LC/MS. High permeability predicts good human oral bioavailablity. High asymmetry index indicates possible PGP efflux.

**Transporter Inhibition**: Test agent is incubated for 2 hr on either side of the monolayer in the presence and absence of a transporter's inhibitor (such as PGP inhibitor verapamil), and thus interaction with transporters is estimated using the CaCO-2 model.

## Footnotes

1. Balimane, PV. AAPS J. 8:1 (2006); Wessel, MD. J Chem Inf Comput Sci 38:726 (1998)

2. Fogh J. et al. 1977. One hundred and twenty seven cultured human tumor cell lines producing tumors in nude mice. J Natl Cancer Inst 59:221-6.

3. Pinto M et al. 1983. Enterocyte-like differentiation and polarization of the human colon carcinoma cell line Caco-2 in culture. Biol Cell 47:323-30.

4. Hidalgo IT et al. 1989. Characterization of the human colon carcinoma cell line (Caco-2) as a model system for intestinal epithelial permeability. Gastroenterology 96:736-49.

5. Takano M et al. 1998. Interaction with P-glycoprotein and transport of erythromycin, midazolam and ketoconazole in Caco-2 cells. Eur J Pharmacol 358:289-94.

6. Taipalensuu J et al. 2001. Correlation of gene expression of ten drug efflux proteins of the ATP-binding cassette transporter family in normal human jejunum and in human intestinal epithelial Caco-2 cell monolayers. J Pharmacol Exp Ther 299:164-170.

7. Xia CQ et al. 2005 Expression, localization, and functional characteristics of breast cancer resistance protein in Caco-2 cells. Drug Metab Dispos 33:637-43.

8. Brandsch M.1994. Expression and protein kinase C-dependent regulation of peptide/H+ co-transport system in the Caco-2 human colon carcinoma cell line. Biochem J 299:253-60.

9. Thwaites DT. 1993. Transepithelial glycylsarcosine transport in intestinal Caco-2 cells mediated by expression of H+-coupled carriers at both apical and basal membranes. J Biol Chem 268:7640-42.

10. Balimane PV et al. 2006. Current industrial practices of assessing permeability and P-glycoprotein interaction. The AAPS Journal 8: Article 1.

11. Braun A et al. 2000. Cell cultures as tools in biopharmacy. 2000. Eur J Pharm Sci 11:S51-S60.

12. Hubatsch I et al. Determination of drug permeability and prediction of drug absorption in Caco-2 monolayers. 2007. Nat Protoc 2:2111-9.

13. FDA Guidance for Industry. Drug interaction studies - study design, data analysis, and implications for cosing and labeling. September, 2006


# BLOOD BRAIN BARRIER (BBB) PENETRATION

BTS Research offers screening services to assess blood brain barrier (BBB) penetration. The assay employs the primary cultures of Bovine brain derived microvascular endothelial cells (BBDMEC). These cells have been evaluated for BBB penetration assessment.

## 1.0 Method Development & Validation

- The sponsor will provide sufficient quantity of each of the compounds of interest, and will provide the structure and molecular weight of the drugs (salt and free form). The sponsor should supply potential internal standards, if available, otherwise BTS Research will attempt to identify suitable internal standards.
- BTS Research will develop LC/MS analytical methods for quantification of each compound in the appropriate matrix. Method validation includes:
  - LC and MS optimization for compounds and appropriate internal standard
  - Calibration curve linearity (1 batch)
  - Inter-batch precision & accuracy, and sensitivity

| | |
|---|---|
| **Required Lead-time:** | **2 week** |
| **Estimated turnaround time:** | **3-4 weeks** |
| **Pricing*:** | **$2,500 per compound.** If methods are not available, please add $1,500 per compound per day for method development. In majority of cases, we average one day for method development. However, based on the chemistry of the compounds some compounds may require one or two additional days assuming there is no derivative chemistry required for LC-MS-MS detection. If method development exceeds five (5) days the sponsor will be notified in writing in advance to approve additional days. |

## 2.0 BBDMEC Cell Permeability Assay

Bovine brain derived microvascular endothelial cells (BBDMEC) are considered on of the best in vitro models for the blood brain barrier.
The endothelial cells express tight junctions (positive for the proteins ZO-1 and Claudin-1) and transport characteristics (P-gp function) found in the blood brain barrier.

# BBDMEX/Astrocytes Blood Brain Barrier Penetration

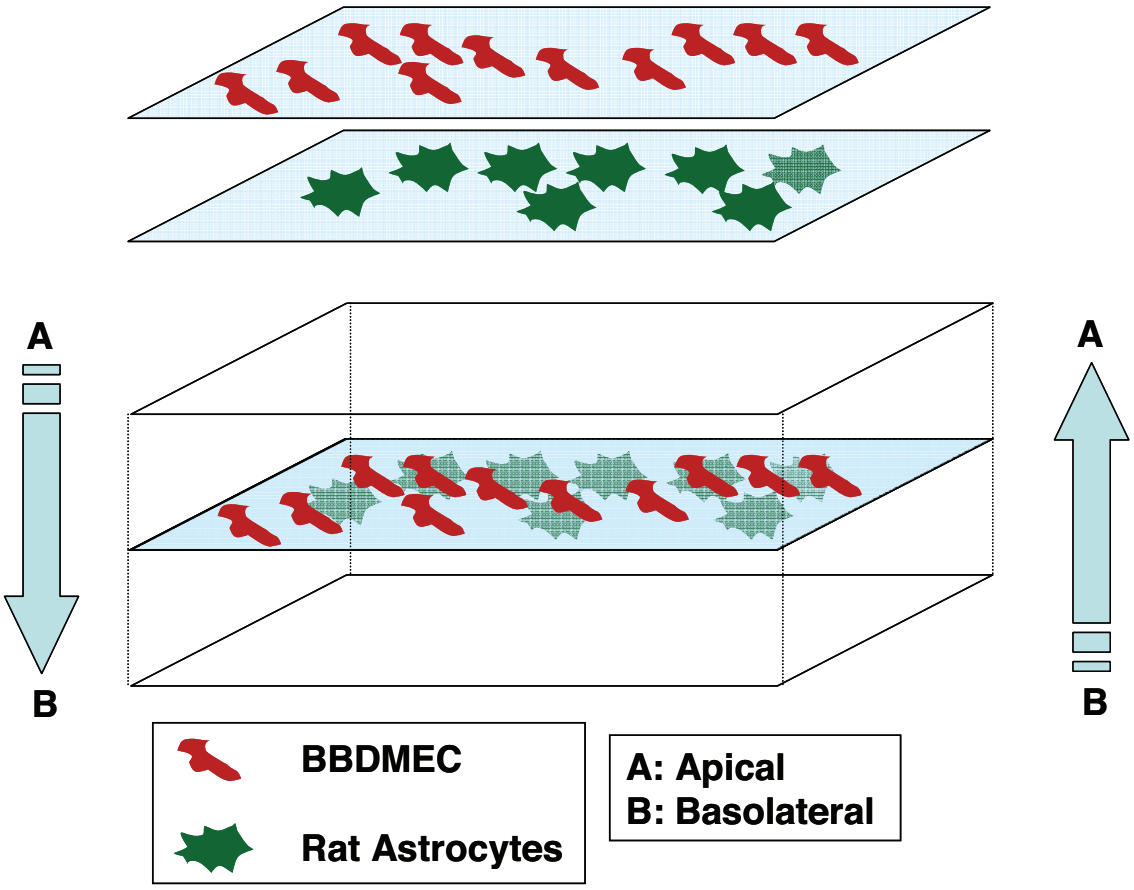


- BBDMEC can be co-cultures with micrgolia cells on the opposite side of the semi-filter
- Cell permeability studies are conducted in 24-well plates.
- The integrity of the cell monolayer is verified by measuring TEER prior to assay.
- Compounds are prepared at one concentration (to be determined in consultation with the client) in 1% DMSO in PBS. Blank controls are used, consisting of 1% DMSO in PBS.
- Lucifer yellow or other standards are used in control wells.
- Each test compound and control is assayed in single in the apical to basolateral direction (A⇒B) and, basolateral to apical direction (B⇒A).
- Two (2) aliquots are sampled from each donor compartment (at the beginning and end), and two (2) aliquots are sampled from each receiver compartment at 1 time-points at 37°C on a rotary shaker.
- Samples containing drug candidates will be analyzed by LC/MS.
- A written report containing a description of the methodology used and summary of results will be provided.

**Required Lead-time:** **2 week**
**Estimated turnaround time:** **4 weeks**
**Pricing*:** **$600** **for 1 compound (minimum of 6 compounds)**

## 3.0 Pricing Proposal

- All prices are shown in US dollars.
- This quotation is valid for a period of 30 days.

The project will be invoiced as follows:

| | % Invoiced | Payment Terms |
|---|---|---|
| Upon acceptance of quotation: | 60% | Due upon receipt |
| Upon submission of raw data | 30% | Due upon receipt |
| Upon submission of final report | 10% | Due upon receipt |

The final report will be submitted upon receipt from Sponsor of comments on draft report, or thirty (30) days after submission of draft report, whichever is earlier.

This proposal is based on the study parameters as described. Many variables are available for modification to ensure that specific Sponsor's objectives are met. These modifications may result in changes to pricing and expected turn around times, depending upon the nature of the modification. If any unusual challenges are encountered during these studies that may affect the scope of work, and as a result the pricing, Sponsor will be consulted immediately. In this event, authorization of any changes to the scope of work and the pricing will be obtained prior to continuing.